hydrology

MDPI

Article

Simulating Groundwater Potential Zones in Mountainous Indian Himalayas—A Case Study of Himachal Pradesh

Anshul Sud [1], Rahul Kanga [1], Suraj Kumar Singh [1,*], Gowhar Meraj [1], Shruti Kanga [2], Pankaj Kumar [3,*], AL. Ramanathan [4], Sudhanshu [1] and Vinay Bhardwaj [5]

1 Centre for Climate Change and Water Research (C3WR), Suresh Gyan Vihar University, Jaipur 302017, India
2 School of Environment and Earth Sciences, Department of Geography, Central University of Punjab, Bhatinda 151401, India
3 Institute for Global Environmental Strategies, Hayama 240-0115, Japan
4 School of Environmental Sciences, Jawaharlal Nehru University, New Delhi 110067, India
5 State Groundwater Department, Government of Rajasthan, Jaipur 302004, India
* Correspondence: suraj.kumar@mygyanvihar.com (S.K.S.); kumar@iges.or.jp (P.K.)

Abstract: Groundwater resources are increasingly important as the main supply of fresh water for household, industrial, and agricultural activities. However, overuse and depletion of these resources can lead to water scarcity and resource deterioration. Therefore, assessing groundwater availability is essential for sustainable water management. This study aims to identify potential groundwater zones in the Bilaspur district of Himachal Pradesh using the Multi Influencing Factor (MIF) technique, a modern decision-making method widely used in various sectors. Geospatial models were integrated with the MIF technique to evaluate prospective groundwater areas. Grid layouts of all underground water influencing variables were given a predetermined score and weight in this decision-making strategy. The potential groundwater areas were then statistically assessed using graded data maps of slope, lithology, land-use, lineament, aspect, elevation, soil, drainage, geomorphology, and rainfall. These maps were converted into raster data using the raster converter tool in ArcGIS software, utilizing Survey of India toposheets, SRTM DEM data, and Resourcesat-2A satellite imageries. The prospective groundwater zones obtained were classified into five categories: nil–very low, covering 0.34% of the total area; very low–low (51.64%); low–moderate (4.92%); moderate–high (18%) and high–very high (25%). Scholars and policymakers can collaborate to develop systematic exploration plans for future developments and implement preservative and protective strategies by identifying groundwater recharge zones to reduce groundwater levels. This study provides valuable insights for long-term planning and management of water resources in the region.

Keywords: MIF technique; remote sensing; groundwater-potential zones; GIS

Citation: Sud, A.; Kanga, R.; Singh, S.K.; Meraj, G.; Kanga, S.; Kumar, P.; Ramanathan, A.; S.; Bhardwaj, V. Simulating Groundwater Potential Zones in Mountainous Indian Himalayas—A Case Study of Himachal Pradesh. *Hydrology* **2023**, *10*, 65. https://doi.org/10.3390/hydrology10030065

Academic Editors: Amimul Ahsan and Peiyue Li

Received: 30 January 2023
Revised: 25 February 2023
Accepted: 7 March 2023
Published: 10 March 2023

1. Introduction

Subsurface water is a critical component of the water cycle, and it is found in rock formations, pores, and cracks beneath the Earth's surface [1,2]. Assessing its potential and preventing water pollution are crucial for maintaining sustainable groundwater resources [3–6]. Groundwater is the largest available freshwater supply in the world, and it is essential for human and ecosystem health as well as economic development [7–11].

In India, groundwater is a major source of water for daily requirements of most of the population [12]. However, several factors, such as industrial growth, increased agricultural output, poor management, and uncontrolled groundwater exploitation, have led to a shortage of potable water [13]. The groundwater potential of an area depends on various factors and it fluctuates as conditions change [14–16]. To counteract groundwater deficits, satellite data can be used to define groundwater prospect zones and expand artificial recharge initiatives [17,18].

Remote sensing (RS) and Geographic Information System (GIS) techniques have proven to be useful in managing aquifer reserves. The reliability of these methods depends on the classification standard and average ranks enforced upon the input parameters [19,20]. Ancillary data, such as toposheets and Landsat images, have enabled the creation of thematic maps using a weighted overlay approach to define potential groundwater zones [21,22].

Various standard approaches have been used to generate statistics about groundwater potential in diverse places with varying meteorological and geographic variables. These approaches include the Analytical Hierarchy Process (AHP), Artificial Neural Network (ANN), Evidential Belief Function Model (EBFM), Electrical Resistivity (ER), Multi-Influencing Factor (MIF), and probabilistic models such as the Frequency Ratio (FR) method [23–25].

While some studies focused solely on lineaments for groundwater exploration, others included additional criteria, such as surface geology, rainfall, lithology, drainage density, lineament density, hydrogeology, soil type, fractional impervious surface, proximity to surface water bodies, and land use/land cover [26–28].

The Groundwater Potential Index (GWPI) is a dimensionless quantification index method that uses themed maps to process potential groundwater scores for distinct locations [29,30]. Using ArcGIS, the research region's groundwater potential map (GPM) can be created by merging all thematic levels of affecting elements [31]. Groundwater prospect zoning has been conducted worldwide [32–38], including in various parts of India, such as Bengal, Chhattisgarh, Orissa, Maharashtra, Tamil Nadu, and others [39–45]. For example, a study by Singha et al., (2019) used GWPI to identify potential groundwater zones in the Chhattisgarh state. The study showed that GWPI can effectively identify groundwater potential zones, and the results were verified by comparing them with well data [46]. Similarly, a study by Dwivedi et al., (2021) used GWPI to assess the groundwater potential of the Betul–Chhindwara Region, in Madhya Pradesh. The study found that the area had a high potential for groundwater development and recommended further exploration and development of groundwater resources in the region [47]. These studies highlighted the usefulness of GWPI in assessing groundwater potential zones in India and demonstrated its potential for improving groundwater management in the country. However, very few studies have been conducted in the Himalayan region [48,49].

The objective of this study is to identify groundwater potential zones in the Bilaspur district of Himachal Pradesh by incorporating MIF, RS, and GIS techniques. The study aims to analyze various influencing factors that affect groundwater potential, including lithology, geomorphology, land use/land cover, slope, and drainage density. Additionally, the study seeks to create a groundwater potential map of the study area by merging all thematic levels of affecting elements using ArcGIS.

The findings of this study can guide policymakers and water resource managers in developing sustainable groundwater management practices and promoting artificial recharge initiatives to counteract groundwater deficits. Previous studies in India have shown the usefulness of GWPI in assessing groundwater potential zones and improving groundwater management practices. This study's results can contribute to the body of knowledge on groundwater management in India and assist policymakers in making informed decisions regarding water resource management.

2. Study Area

Himachal Pradesh, is one of the northernmost states of India, nestled in the lap of the Western Himalayas. Himachal Pradesh is a diverse state with a variety of geographical areas and subregions, each with its own climate, vegetation, and fauna. On account of its location and topography, the state has a wide range of climates. The state's climate ranges from warm temperatures in the lower Shivalik plains to semi-arctic cold temperatures in the Kullu and Chamba valleys, with temperate climate conditions in Kinnaur and the Lahaul–Spiti alpine regions [50]. This study has been carried out in the Bilaspur district. The Shivalik range in the lower Himalayas encompasses this district, which covers 2.1 per cent of the state's land, around 1167 km^2 (Figure 1). The district is primarily

traversed by the Satluj River, which deposits alluvial materials. The study area is located at an average elevation of 610 m between latitude 31°18′ N and 31°55′ N and longitude 75°55′ E and 76°28′ E. The rural citizenry of the study region comprises around 93 per cent of the population, with a density of 327 people per square kilometre. With more than 70% of the population involved in agriculture and allied businesses, agriculture is the most popular occupation in the area. The climate in the study region is characterized by warm summers and chilly winters. However, its location in a valley protects it from the temperature extremes of the surrounding mountains. May and June are the hottest months, with temperatures occasionally reaching 40 °C. December and January are the coldest, with temperatures sometimes falling below 0 °C [51]. In addition, the economy of the region is heavily dependent on agriculture and groundwater plays a vital role in supporting agricultural activities [52]. Therefore, assessing the availability and potential of groundwater in the area is not only important for ensuring a sustainable water supply, but also for supporting the economic viability of the region [53].

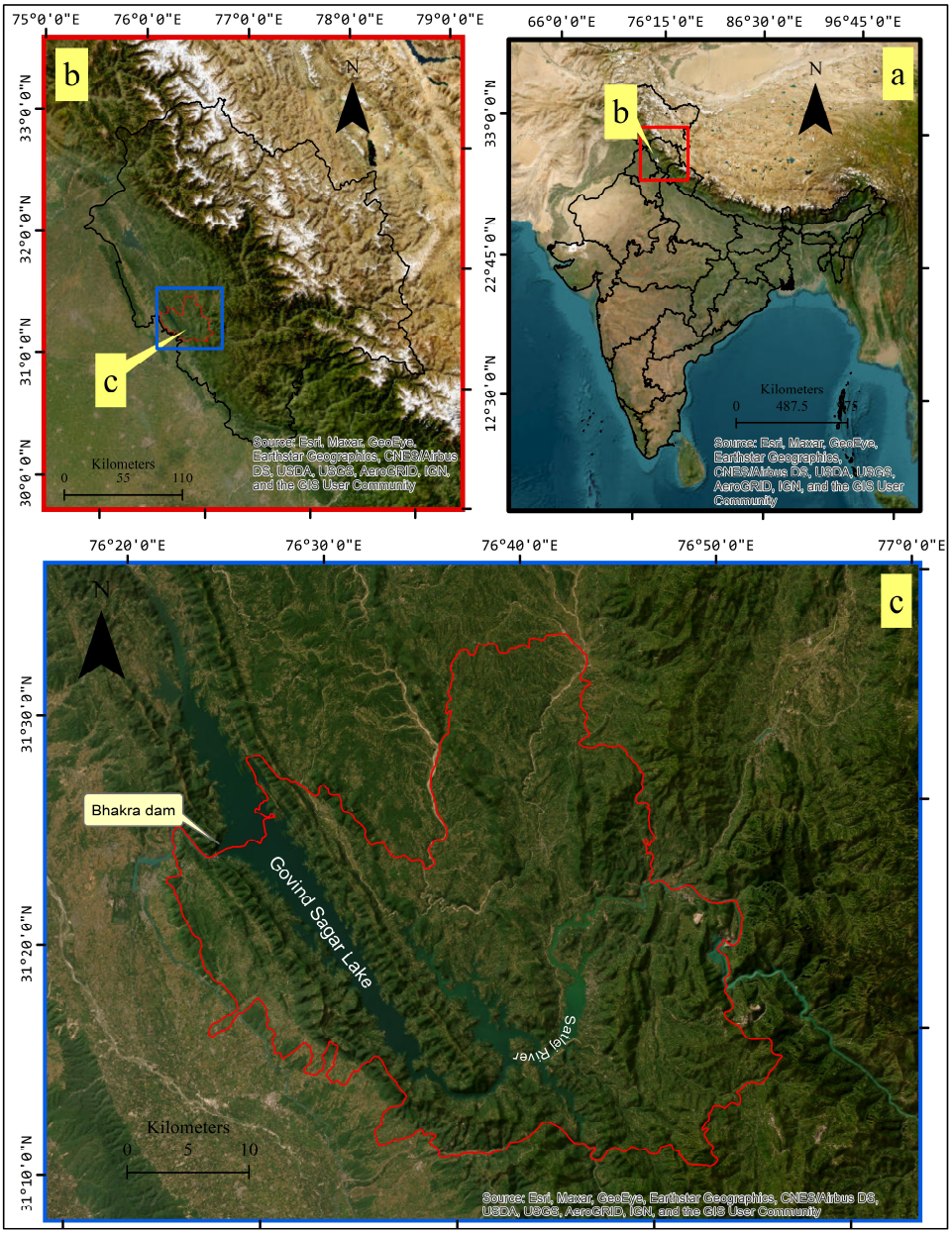

Figure 1. Location of the study area. (**a**) India, (**b**) Himachal Pradesh, and (**c**) Bilaspur District. Map coordinates are in UTM Zone 43.

The Bilaspur district receives an average of 1100 mm precipitation annually, with the monsoon season being the primary contributor. The area is predominantly covered with sedimentary rocks, and the soil profile on river terraces along the Satluj ranges from 1 to 3 m, with mostly alluvial and loamy soil except for clayey patches. In the Bilaspur district of Himachal Pradesh, India, Govind Sagar Lake is a significant attraction [54]. The lake is a vast artificial reservoir formed by the Bhakra Dam, which is one of the largest dams in India, constructed across the Sutlej River in the mid-20th century [55]. The lake spans an area of approximately 170 km^2 and has a storage capacity of 9.34 billion cubic meters. The economic and social development of the Bilaspur district and the surrounding areas has been significantly influenced by the Govind Sagar Lake, and it continues to be an essential resource for the local community and a popular tourist destination.

3. Materials and Methods

3.1. Dataset Used and Preparation of Thematic Maps

The datasets and methods used in this study are shown in Figure 2. Toposheets obtained from the Survey of India (SOI) at a scale of 1:50,000 were used to demarcate the administrative boundary of the study area. Datasets for deciphering groundwater potential zones are divided into satellite, meteorological, and ancillary data. Resourcesat-2, Linear Imaging Self-Scanning Sensors (LISS)—III imagery with a spatial resolution of 23.5 m, downloaded from the Bhuvan portal (http://bhuvan.nrsc.gov.in/ accessed on 31 February 2021) for this investigation was used to prepare land use/landcover, and geomorphology. We used a supervised classification approach to map land use and land cover (LULC) and visual image interpretation for geomorphological mapping of the study area [56–62]. For lineament mapping, we employed an integrated approach that involved both automated algorithms, such as edge detection, lineament extraction, or curvature analysis, and visual interpretation of the Landsat image and digital elevation model (DEM) data [63,64]. This approach helped us identify and map linear features in the study area with greater accuracy.

We prepared aspect, slope, drainage density, and elevation maps using Shuttle Radar Topography Mission (SRTM) digital elevation model (DEM) data with a global resolution of 1 arc-second, acquired from USGS EarthExplorer. Standard GIS methods were used to prepare these datasets, and the spatial analyst tool of the ArcGIS suite was used to generate the aspect, slope, drainage density, and elevation maps. The SRTM DEM data provided the necessary information to compute the terrain characteristics, such as aspect and slope, while the drainage density and elevation maps were derived from the computed terrain characteristics [58,65]. The aspect map shows the direction of the terrain slope, while the slope map shows the steepness of the terrain [58]. The drainage density map shows the concentration of stream channels in the area, and the elevation map shows the height of the terrain above sea level [62]. The atlases of NBSS and LUP (National Bureau of Soil Surveying and Land Use Planning) were used to construct the soil map [62]. Geological Survey of India's (GSI) data was used to construct the lithology map [66], and the rainfall map was created with data from the India Meteorological Department (IMD), Pune, by employing the inverse distribution weighted (IDW) approach.

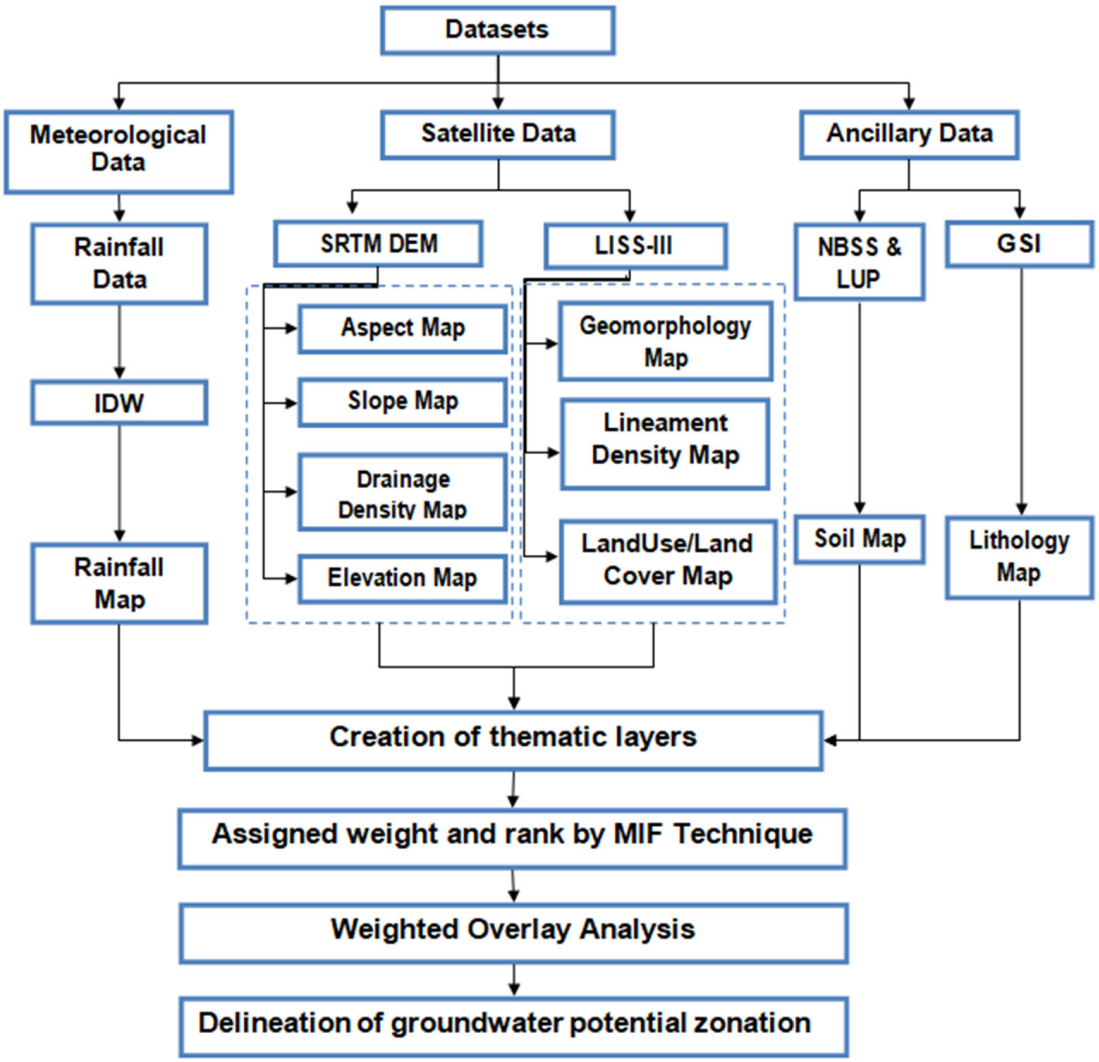

Figure 2. Methodology flowchart used in the study.

3.2. Calculation of Weightage of MI Factors for Zonation of Groundwater Potential

Multi-influencing parameters have been recognized to decipher potential groundwater zones, such as lineament density, drainage density, land-use/landcover, aspect, slope, elevation, soil, rainfall, lithology, and geomorphology [22,30,40,42–45]. Depending on the circumstances, each influencing factor's effect may contribute to identifying potential groundwater zones. More crucially, these elements are intertwined, and their effect is shown in Figure 3.

In the MIF technique, data layers are set and each primary and secondary factor is assigned an influence of m times and 0.5 m times, respectively. The total weights from the respective component make up a factor's representative weight in the potential zone. Each influencing factor's grade is then determined using the following algorithm and later integrated using weighted overlay analysis.

$$(G + H) \times 100/\Sigma(G + H), \quad (1)$$

where G is the major nexus among two parameters and H is the minor interdependence between two factors. As shown in Table 1, a roughly equivalent share of the pertinent score was awarded to individual reclassified parameters [42–45]. Each influential contributor received an equal amount of the associated score for each reclassified parameter (Table 2).

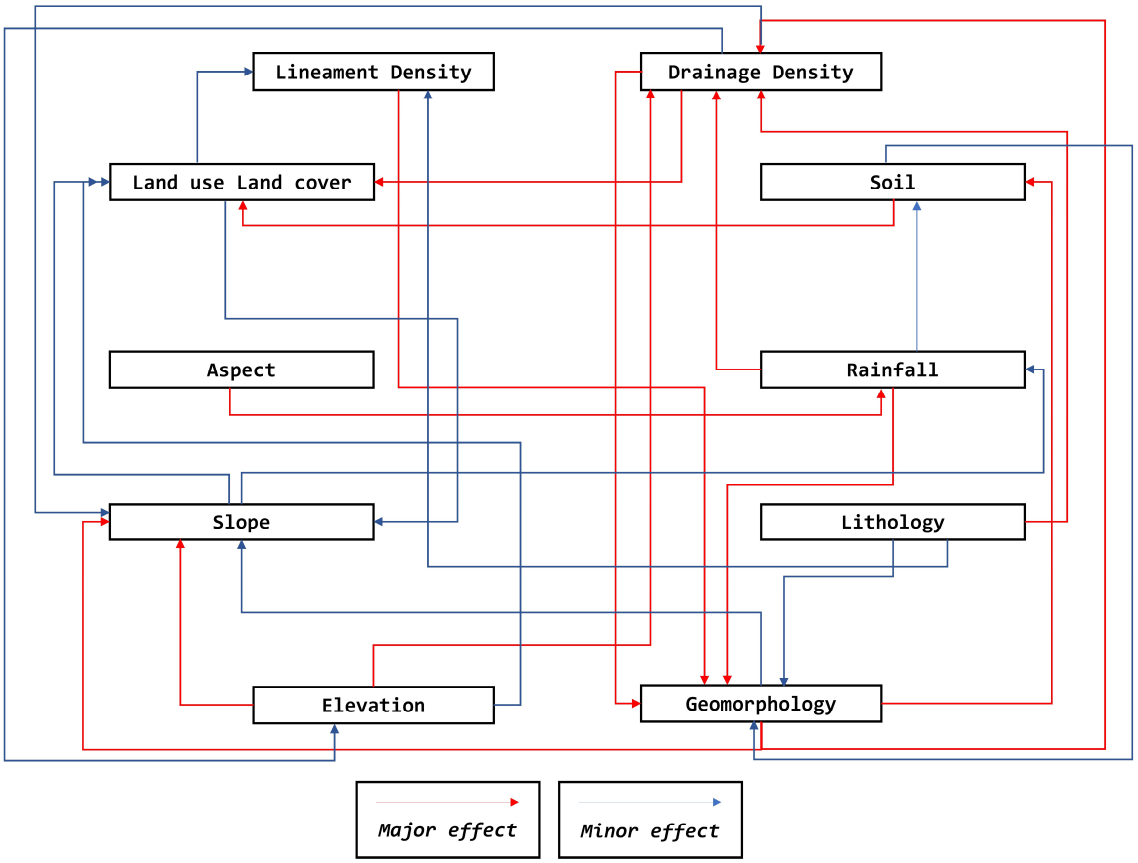

Figure 3. Diagram showing multi-influence factors for potential groundwater zones.

Table 1. Impact of influencing factor, proposed score, and each potential factor's relative rates.

Factor	Major Effect (G)	Minor Effect (H)	Proposed Relative Rates (G + H)	Proposed Score of Each Influencing Factor
Drainage Density	2	1	3	13
Lineament Density	2	0.5	2.5	11
LULC	1	0.5	1.5	6
Aspect	1	0	1	4
Slope	1	1	2	9
Elevation	2	0.5	2.5	11
Soil	1	0.5	1.5	7
Rainfall	2	0.5	2.5	11
Lithology	2	1	3	13
Geomorphology	3	0.5	3.5	15
Total			23	100

Table 2. Weight factors' categorisation of influencing zones of potential groundwater.

Factor	Descriptive Scale	Weight (a) 1–10	Domain of Effect	Rate (b) 1–4	Weighted Rating (a × b)	Total	Average Weight (a × b/∑a × b) × 100
Drainage density	<0.5	9	HVH	3	27	75	11
	0.5–1.0	7	MH		21		
	1.0–1.5	5	LM		15		
	1.5–2.0	3	VLL		9		
	>2.0	1	NVL		3		
Lineament density	<0.3	1	NVL	2.5	2.5	62.5	9
	0.3–0.6	3	VLL		7.5		
	0.6–0.9	5	LM		12.5		
	0.9–1.2	7	MH		17.5		
	>1.2	9	HVH		22.5		
LU/LC	Waterbody	9	HVH	1.5	13.5	81	11
	Cropland	9	HVH		13.5		
	Forest Evergreen	7	MH		10.5		
	Forest Scrub	7	MH		10.5		
	Forest Deciduous	7	MH		10.5		
	Grazing land	6	MH		9		
	Scrubland	4	LM		6		
	Ravenous land	3	VLL		4.5		
	Built-up Land	2	VLL		3		
Aspect	North	9	HVH	1	9	44	6
	North-east	8	HVH		8		
	East	7	MH		7		
	North-west	6	MH		6		
	West	4	LM		4		
	South-east	5	LM		5		
	South-west	3	VLL		3		
	South	2	VLL		2		
	Flat	1	NVL		1		

Table 2. *Cont.*

Factor	Descriptive Scale	Weight (a) 1–10	Domain of Effect	Rate (b) 1–4	Weighted Rating (a × b)	Total	Average Weight (a × b/∑a × b) × 100
Slope (degree)	<10	9	HVH	2	18	62	9
	10–20	7	MH		14		
	20–30	6	MH		12		
	30–40	5	LM		10		
	40–50	3	VLL		6		
	>50	1	NVL		2		
Elevation (meters)	<550	9	HVH	2.5	22.5	75	11
	550–750	7	MH		17.5		
	750–950	6	MH		15		
	950–1150	5	LM		10		
	1150–1350	3	LLV		7.5		
	>1350	1	NVL		2.5		
Soil	Sandy	9	HVH	1.5	13.5	34.5	5
	Coarse loamy	7	MH		10.5		
	Loamy	5	LM		7.5		
	Fine loamy	2	VLL		3		
Rainfall (mm)	<1350	2	NVL	2.5	5	64.5	9
	1350–1450	3	VLL		7.5		
	1450–1550	5	LM		12		
	1550–1650	7	MH		17.5		
	>1650	9	HVH		22.5		
Lithology	Alluvium deposit	9	HVH	3	27	114	16
	Upper Shiwalik	7	MH		21		
	Lower Shiwalik	5	LM		15		
	Shali	5	LM		15		
	UndifferentialSubathu	3	VLL		9		
	Middle Shiwalik	3	VLL		9		
	Dagshai formation	3	VLL		9		
	Kakara formation	3	VLL		9		
Geomorphology	Structural hills	3	VLL	3.5	10.5	92.5	13
	Denudational hill	6	LM		19		
	Valley fill	9	HVH		31.5		
	Reservoir	9	HVH		31.5		

NVL Nil *Very-Low*, VLL *Very Low-Low*, LM *Low-Moderate*, MH *Moderate-High*, HVH *High-Very High*.

4. Results and Discussion

The data for multi-criteria decision-making analysis were obtained from the satellite imageries, climatic, and conventional data acquisition methods, and several thematic layers were created using ArcGIS software. Different thematic layers are described and illustrated below.

4.1. Analysing Drainage Density

The ratio of a stream's entire length (l) to the total area of the basin is known as drainage density and is represented by Dd. It is a measure of a drainage basin's hydrograph form and is an important statistic for determining subsurface water potential areas [24]. A lower Dd indicates lower surface runoff as well as strong water infiltration, signifying great vegetation coverage and increased groundwater recharge, whereas a higher Dd suggests the opposite [65–67]. Undulating hilly terrain with canyons and passes covers the entire region.

Along with numerous seasonal streams, the study region is also home to about four perpetual streams (Figure 4a). Five groups have been created from the drainage density values (km/km^2) of the study area. The areas are categorized as nil–very low (>2.0), indicating 0.14% area, very low–low (1.5–2.0) representing 1.3% area, low–moderate (1.0–1.5) representing 3.8% area, moderate–high (0.5–1.0) representing 30% area, and high –very high (<0.5), accounting for 65% of the overall study area (Figure 4b).

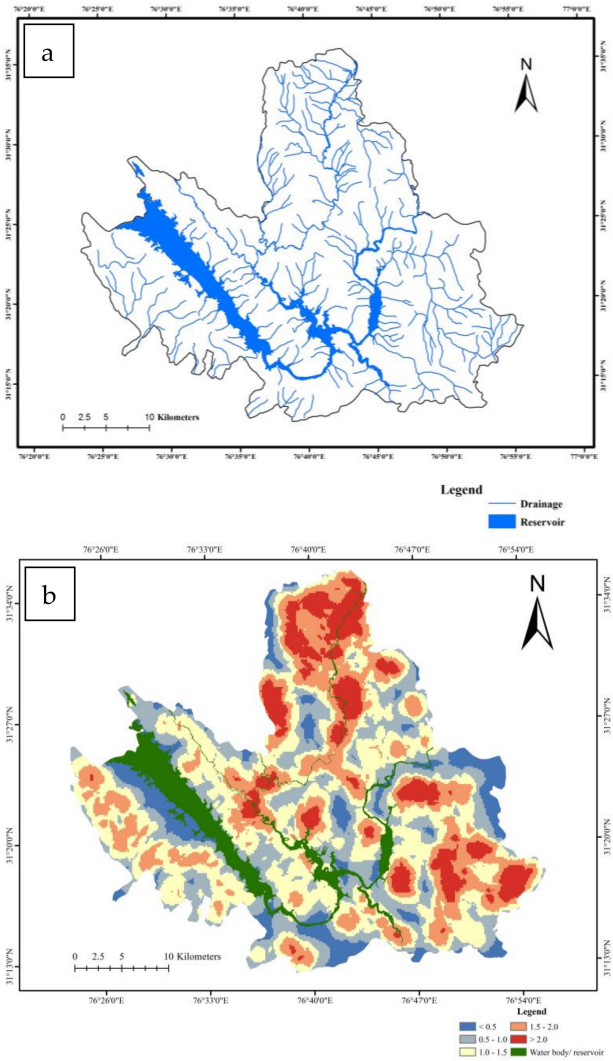

Figure 4. (**a**) Drainage map of Bilaspur district; (**b**) Drainage density map of Bilaspur district.

4.2. Lineament Density Analysis

Lineaments have an important role in recharging groundwater in mountainous territories. Since the existence of lineaments usually shows signs of a pervious zone, lineament density in a region may indirectly indicate the potential for groundwater [26]. Groundwater potential zones benefit from high lineament density [63]. The majority of lineament has been discovered at various angles along the NW direction, with only a few along North-South and East-West directions (Figure 5a).

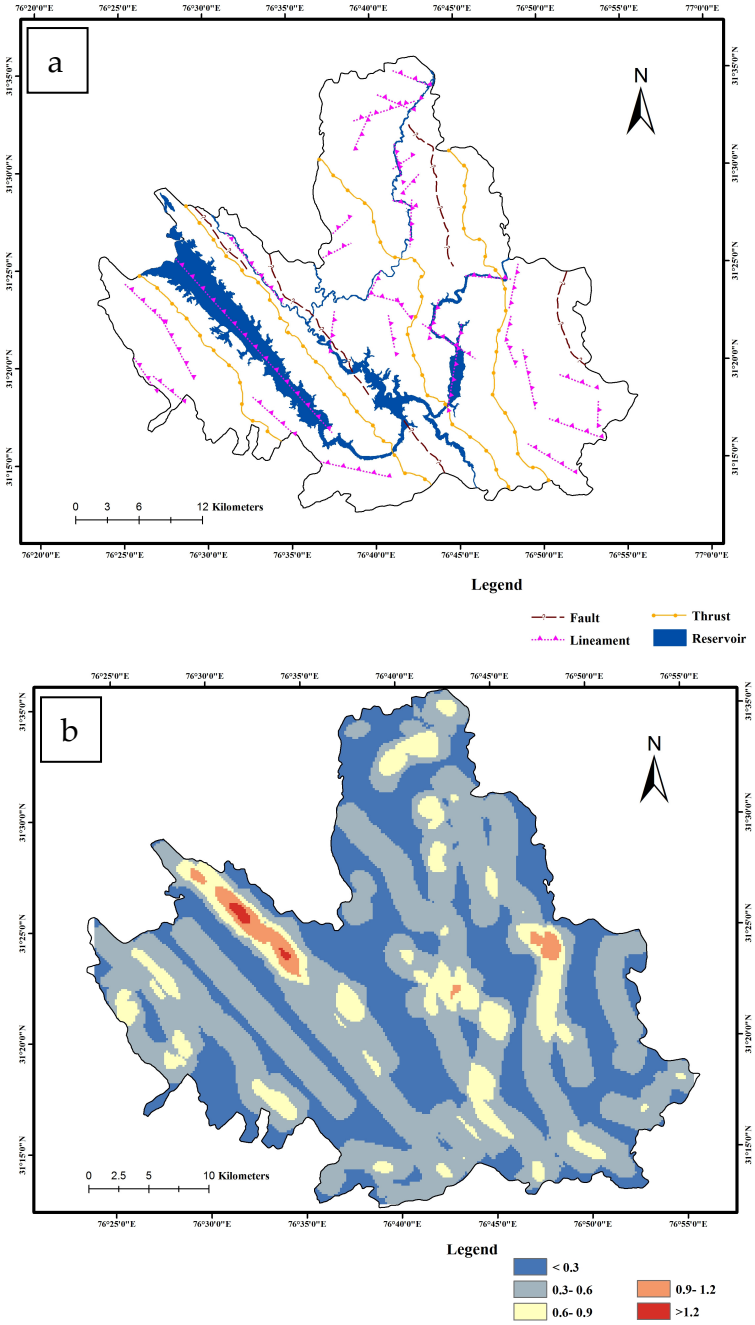

Figure 5. (**a**) Structure map of Bilaspur district; (**b**) Lineament density map of Bilaspur district.

High–very high (>1.2) and moderate–high (0.9–1.2) are those classifications (out of five) for lineament density levels (km/km^2) that have no significant impact. The low–moderate group ranges from 0.6 to 0.9 represents 10.5% area, while very low–low (0.3–0.6) and nil–very low (<0.3) jointly account for more than 88% of the overall study area [Figure 5b].

4.3. Land Use and Land Cover Analysis

The groundwater potential in a given location is heavily impacted by land use/land cover (LULC). The maximum likelihood algorithm technique was used to classify the land use/land cover map (Figure 6a) created from a LISS III sensor multispectral image. Waterbody, scrubland, ravenous land (barren), grazing land, built-up land, cropland, forest scrub, forest evergreen, and forest deciduous are among the nine categories of LU/LC found in the research region.

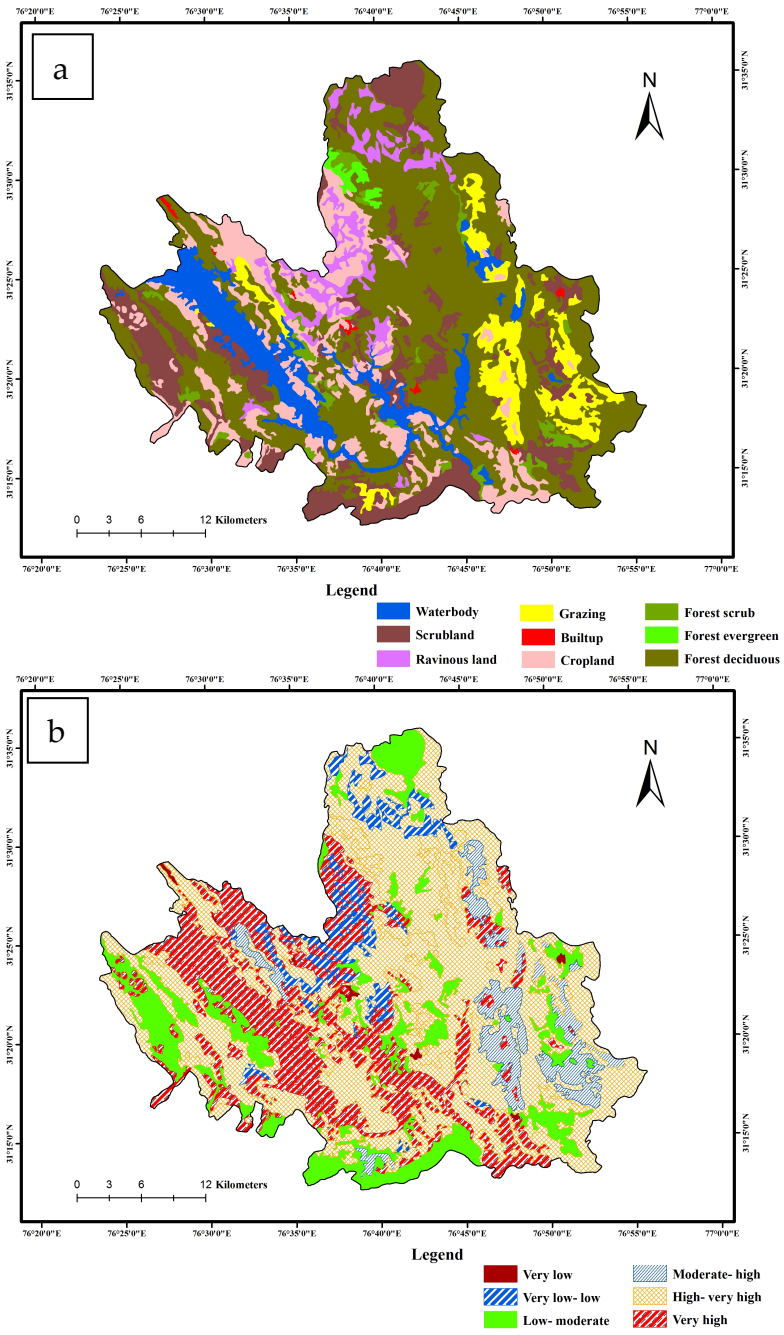

Figure 6. (**a**) Land use/land cover map of Bilaspur district; (**b**) LU/LC index map of Bilaspur district.

Suitable weighting was awarded to different land use/land cover classes on the basis of their water requirements. By serving as aquifer recharge zones, waterbodies such as lakes, rivers, and ponds can increase the groundwater potential [62]. Waterbodies serve as a direct supply of groundwater in regions with shallow groundwater tables. Consequently, this category was given the HVH index (Figure 6b). Depending on the sort of irrigation

technique utilized, croplands may have an impact on groundwater potential. Irrigation may recharge the groundwater if water is applied in the proper quantity and at the right time. Hence, this category was assigned an HVH index. By boosting infiltration and reducing the rate of surface runoff, forests can improve the groundwater potential. Trees in forests can absorb a substantial amount of water from the soil and transpire it back into the atmosphere, slowing the rate of groundwater recharge [24,62]. As a result, the MH index was given to this group. Pastures are a common feature of grazing areas, and they help speed up infiltration and improve groundwater potential [62,66]. As a result, this category was given the MH index. Deep-rooted plants found in scrublands can improve infiltration and rehydrate the groundwater [62,66]. As a result, this category was given an LM index. Limited vegetation coverage and rainfall in ravenous land (barren) environments, such as deserts and arid areas, result in low groundwater potential [24,62,66]. As a result, this category was given a VLL index. Cities and other densely populated regions have the potential to lower groundwater levels by accelerating surface runoff and stifling infiltration. Roads, walkways, and parking lots with paved surfaces can stop precipitation from accessing the soil, limiting recharge [56]. As a result, this category was given a VLL index.

Forests and cropland account for 50.2% of the total land area, grazing land covers 6.9%, and scrubland represents 15%. Due to the lack of vegetation and impermeable nature, ravenous land and built-up areas constitute 5% of the research region (Figure 6b).

4.4. Aspect Analysis

Local climate is strongly influenced by aspect, a significant influencing characteristic that impacts an area's groundwater recharge potential. This is due to the sun's angle being less than 90 degrees in both hemispheres (North and South) or directly overhead. An aspect map was prepared from SRTM DEM (Figure 7a). A west-facing hill will typically be warmer than a protected east-facing slope because sun rays are in the west during the hottest part of the day (unless heavy precipitation influences dictate otherwise) [68].

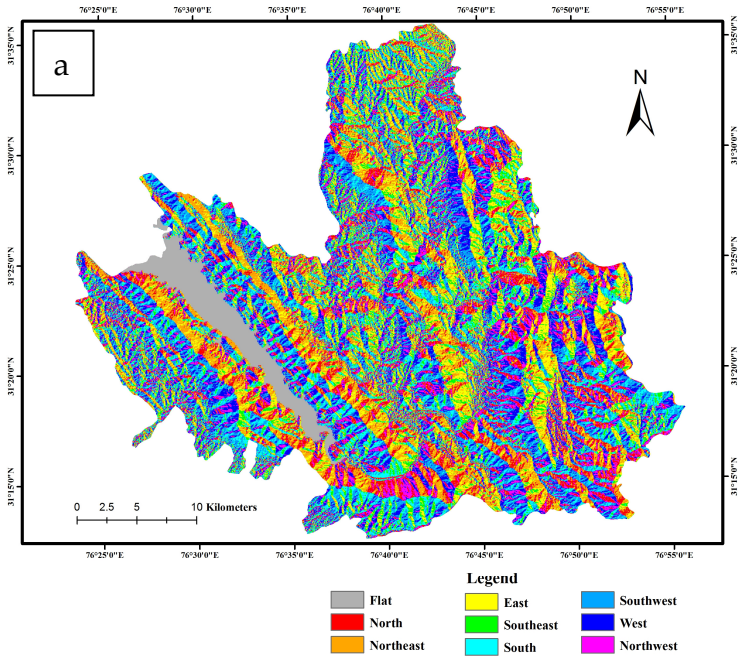

Figure 7. *Cont.*

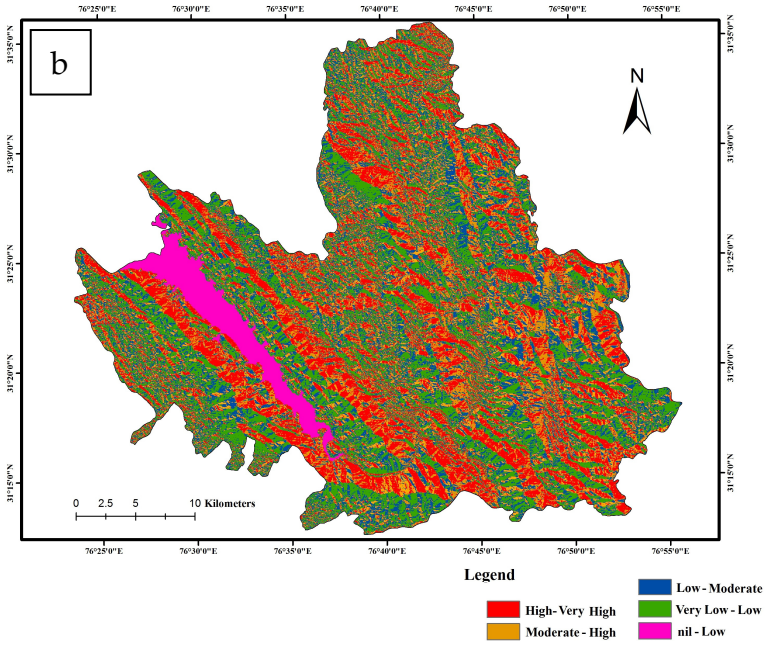

Figure 7. (**a**) Aspect map of Bilaspur district; (**b**) Aspect index map of Bilaspur district.

With relatively high levels of evapotranspiration, a south-facing slope in the northern hemisphere (more susceptible to sunlight and warm winds) will be significantly hotter than a north-facing slope. Flat terrains are given less weight, whereas those heading north are given the most [69]. All regions of the study area have almost equal groundwater potential (Figure 7b).

4.5. Slope Analysis

The availability of groundwater can be reflected by the slope angle; a higher slope portion generates rapid runoff from the terrain and so provides little water for groundwater recharging, while rainfall infiltration and percolation are allowed in lower slope sections of flat terrain, making it suitable for groundwater recharge [24,62,66]. The slope map is created using a digital elevation model (Figure 8a). About 1.44% of the study area comes in >40°, with 91.63% of the area being moderate–high, 3.8% low–moderate, and 3.1% high–very high groundwater potential (Figure 8b).

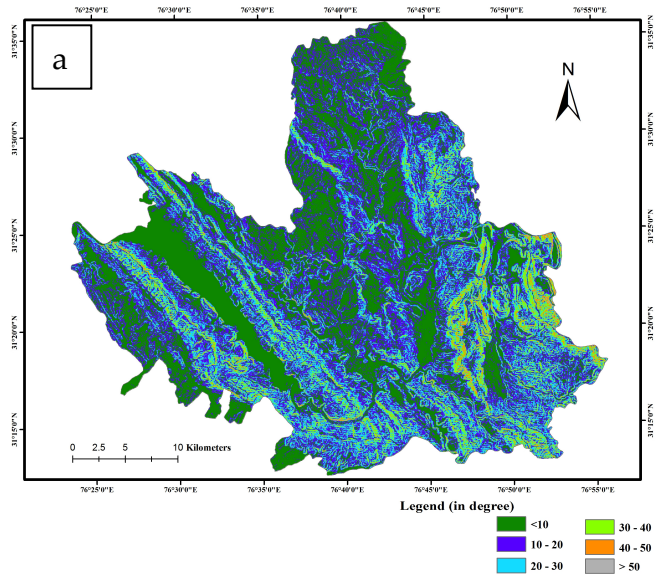

Figure 8. *Cont.*

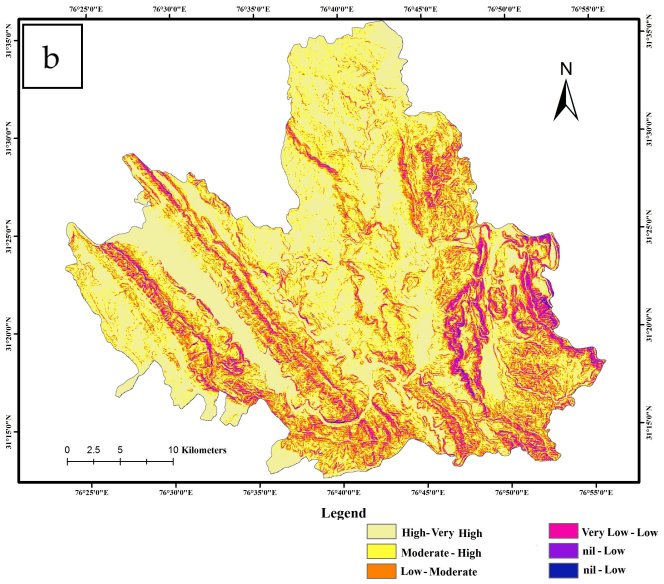

Figure 8. (**a**) Slope map of Bilaspur district; (**b**) Slope index map of Bilaspur district.

4.6. Elevation Analysis

The water level of any research area is influenced by elevation, which is a topographical feature. SRTM DEM was used to construct the elevation map. Due to the infiltration rate, surface runoff, and other factors, higher elevations (>1350 m) receive a lower score, whereas lower altitudes (<550 m) receive a higher rank [Figure 9a]. This is justified by the fact that the topography of the land affects the infiltration rate and surface runoff [24,62,66]. Slopes are often steeper at higher elevations, increasing surface runoff and decreasing infiltration rates. As a result, there is less water available for groundwater recharge, which increases the risk of dangers such as landslides and erosion [25,26,70]. Lower elevations, on the other hand, frequently have kinder slopes and are better suited for infiltration and groundwater recharge. Therefore, they are awarded a better ranking in terms of groundwater potential [70].

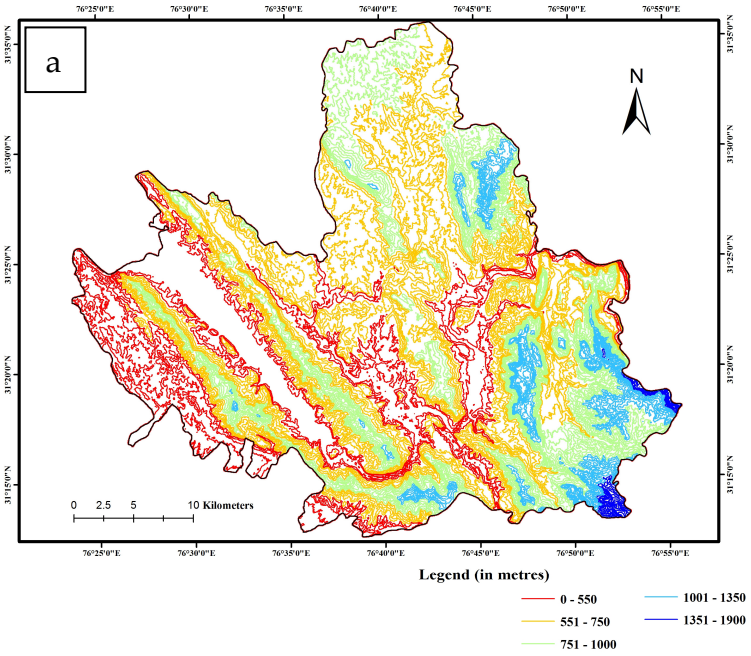

Figure 9. *Cont.*

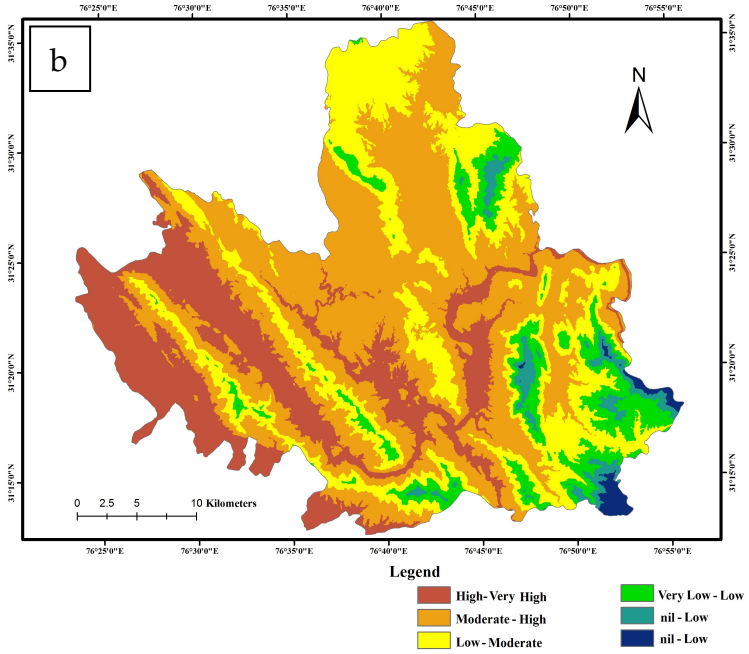

Figure 9. (**a**) Contour map of Bilaspur district; (**b**) Elevation index map of Bilaspur district.

The research area's elevation is classified into six classes. Only 5.3% of the area comes in very high–high, 30.2% area high–moderate, 28.3% moderate–low and 36% low–very low groundwater potential [Figure 9b].

4.7. Soil Analysis

Soil types determine the quantity of water that can seep into subterranean formations and thus impact groundwater recharge [24]. Four soil types were identified and analysed based on their groundwater expectations: coarse-loamy, fine-loamy, loamy, and sandy soil (Figure 10a). Coarse-textured soil types are better suited for infiltration into surface soils because they transport water quickly, but fine-textured soils have limited permeability and small pores that clog quickly [65,66].

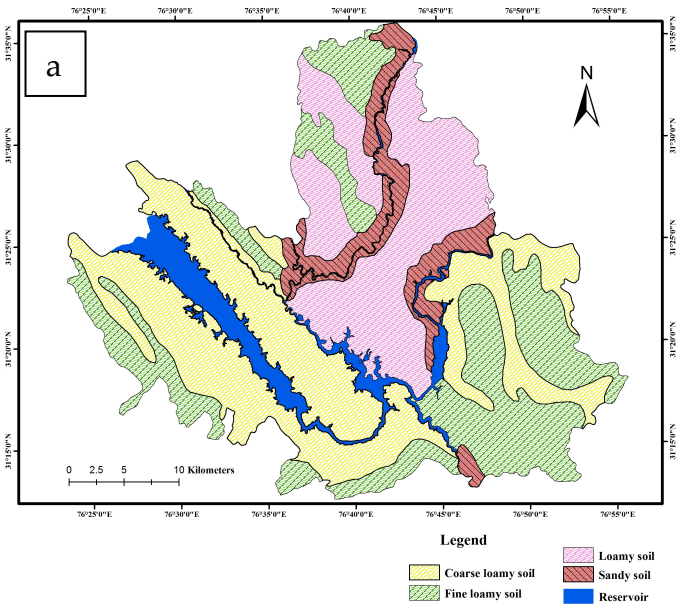

Figure 10. *Cont.*

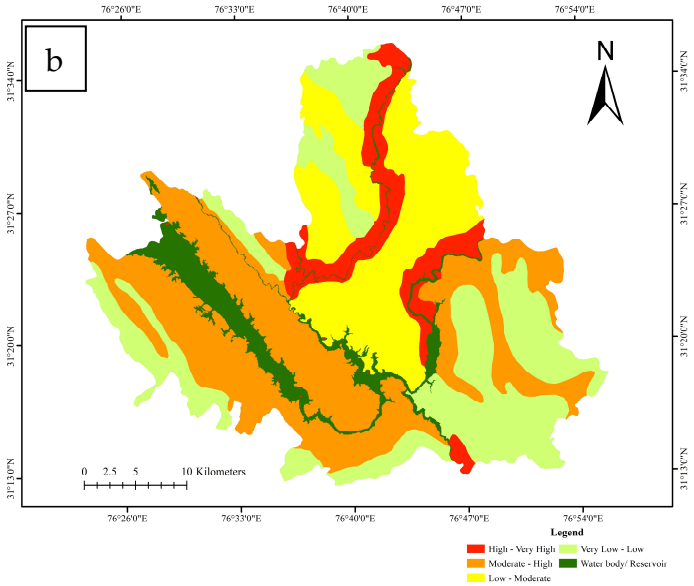

Figure 10. (**a**) Soil map of Bilaspur district; (**b**) Soil index map of Bilaspur district.

Sandy soils are very permeable, light-grained, and well-drained, have excellent infiltration rates, and offer the best prospects for groundwater, hence they receive maximum weight [58]. Due to its coarse texture, coarse clay soil is given the second highest weight, followed by clay soil and, finally, fine clay soil, which is assigned the lowest weight due to its fine texture. The results revealed that 16.1% of the study area has a high–very high groundwater potential. The study region's south-western (33.8%) part is classified as moderate–high, 22.5% as low–moderate, and 27.6% as very low–low groundwater potential (Figure 10b).

4.8. Rainfall Analysis

In terms of groundwater recharge, rainfall is one of the most prominent contributors. The south-east portion of the study area receives less than 1350 mm of rain [Figure 11a]. As we get closer to the district's northern reaches, rainfall intensifies. The penetration rate of runoff water is directly influenced by rainfall distribution and slope gradient, which increases the possibility of groundwater potential zones arising as a result [71].

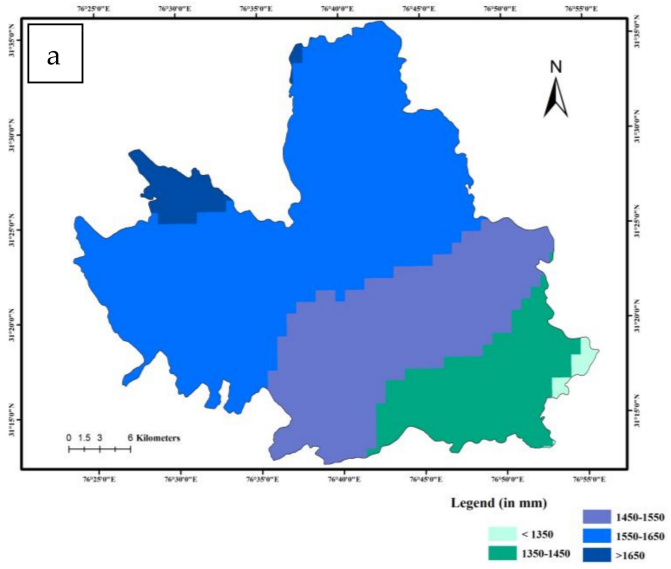

Figure 11. *Cont.*

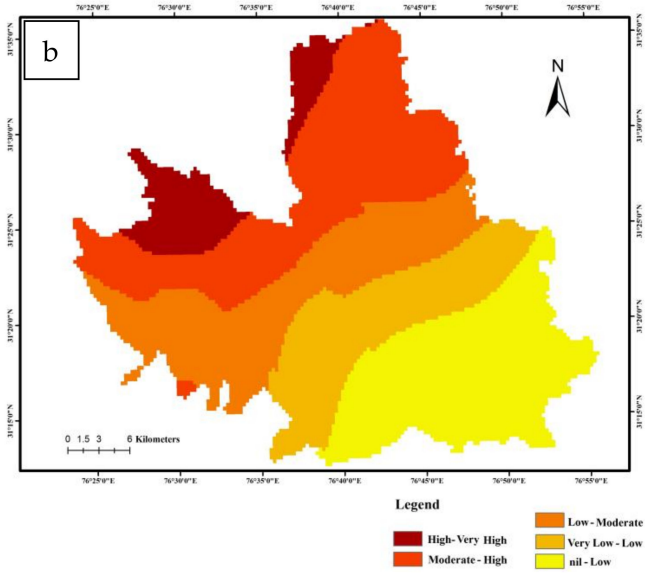

Figure 11. (**a**) Rainfall map of Bilaspur district; (**b**) Rainfall index map of Bilaspur district.

The rainfall map was constructed by employing the inverse distance weighted (IDW) interpolation method in ArcGIS, utilising estimates of mean total yearly rainfall on the basis of various station data [72]. Nil–very low (<1350), very low–low (1350–1450), low–moderate (1450–1550), moderate–high (1550–1650), and high–very high (>1650) are the five categories of rainfall based on upper and lower limits [Figure 11b].

4.9. Lithology Analysis

Lithology plays an essential role in both the porosity and permeability of aquifer materials [73]. The lithology map ranged from very low–low to high–very high, depending on the type of formation, viz., Upper Siwalik, undifferentiated Subathu group, Shali formation, Middle Siwalik, Lower Siwalik, Kakara series, Dagshai formation, and Alluvium deposits (Figure 12a). Sand, silt, clay, gravel, pebbles, and cobbles with high porosity and thus high permeability make up alluvium deposits, which are given the highest weight [66]. Soft sandstone, brownish clay, shale, poorly sorted and crudely bedded conglomerate, and extremely permeable boulder beds make up the Upper Siwalik formations, which are accorded the second greatest weight [66].

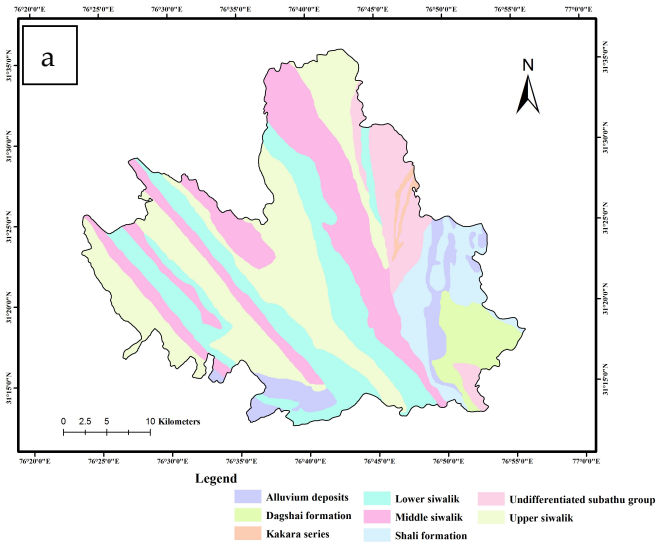

Figure 12. *Cont.*

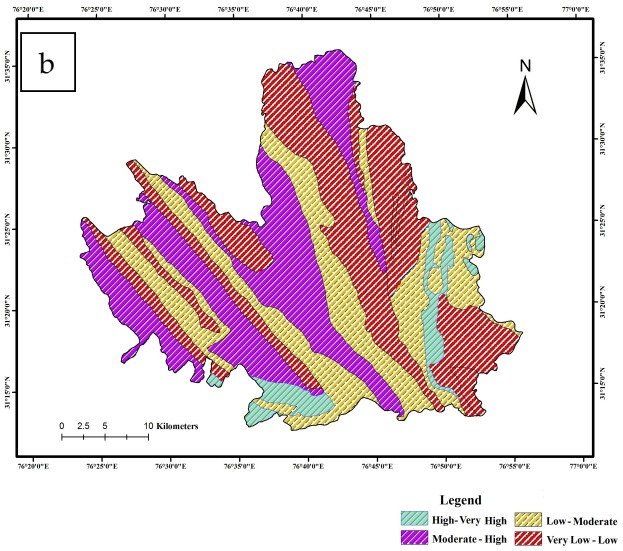

Figure 12. (**a**) Lithology map of Bilaspur district; (**b**) Lithology index map of Bilaspur district.

Due to the presence of well-connected pore spaces, the Lower Siwalik formation is renowned for having a high permeability, which is advantageous for groundwater movement and storage [74]. However, it is also important to take into account any potential contamination brought on by anthropogenic and natural pollutants. Cherty dolomite, quartzite, and limestone make up the Shali formation, and these materials are generally more resistive to groundwater movement due to their lower porosity and permeability [75]. However, groundwater transport and storage may be facilitated by cracks and joints in the formation. Due to the existence of impermeable clay layers, the Dagshai formation has limited permeability [76], which makes it less suited for groundwater movement and storage. However, in places where the shale strata are weaker or fractured, localised groundwater recharge and storage can take place [77]. According to the lithology map, the southern half of the district's alluvial deposits and Lower Siwalik formation have high to very high groundwater potential. However, the Dagshai formation has relatively lower potential because of its lower permeability. The lithology map reveals that 5% of the area containing alluvial deposits in the district's southern part has very high–high, and 27% of the Lower Siwalik area has high–moderate groundwater potential, respectively (Figure 12b).

4.10. Geomorpology Analysis

Different sub-types of geomorphic formations have varying capacities to hold onto water. Structured hills, denudational hills, valley fills, and reservoirs are some of the classifications seen in the study region [78] (Figure 13a). These classes were given varying weights based on their significance in groundwater recharge. Valley fill received the maximum weight because it is close to a reservoir and thus has great potential for recharge, while the least weight was given to structural hills because they primarily produce runoff, as opposed to denudational hills, which produce recharge-cum-runoff, although the recharge is very small.

In the thematic mapping, the geomorphology of our study area has been divided into three categories: the central portion (high very–high), which occupied 42.9% of the total area; low–moderate, which occupied 50.6% of the total area; and moderate–high, which occupied 6.4% of the total area [Figure 13b].

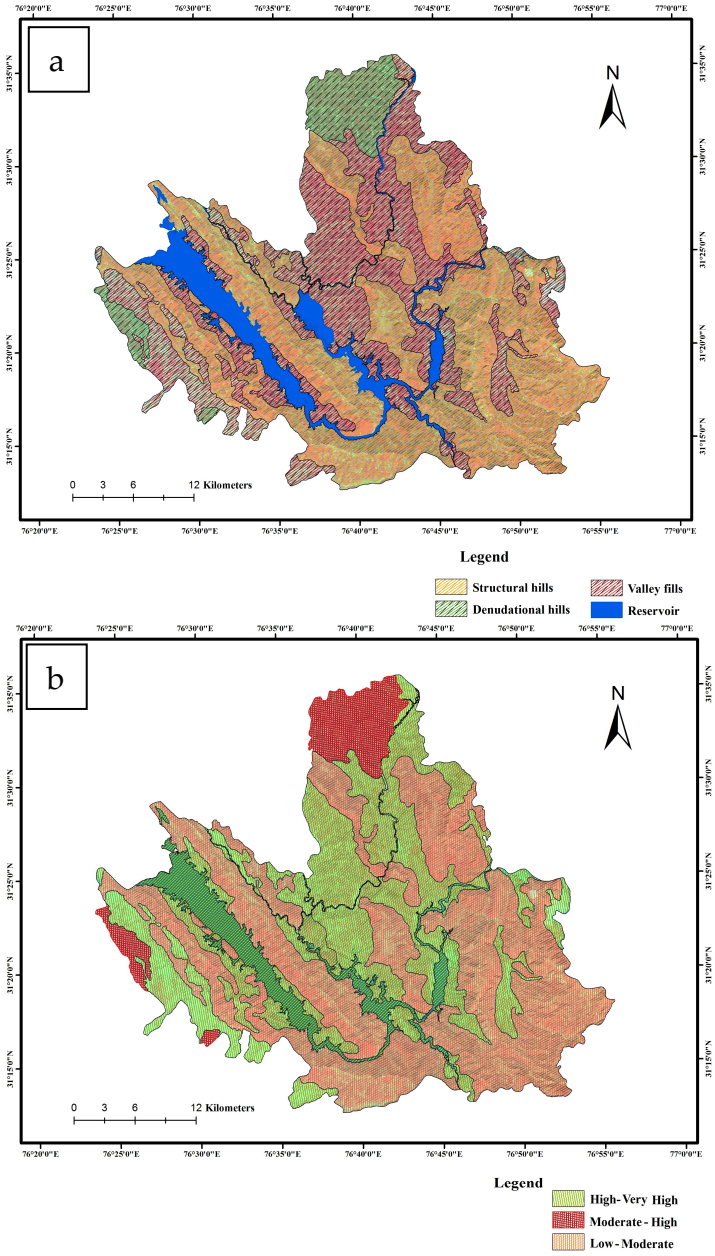

Figure 13. (**a**) Geomorphology map of Bilaspur district; (**b**) Geomorphology index map of Bilaspur district.

4.11. Delineation of Groundwater Potential Zones

The prospective recharge zones for the study area have been created by combining several thematic maps, such as aspect, geomorphology, drainage density, elevation, soil, slope, lithology, rainfall, lineament density, land use, and land cover, into a single map using RS-GIS techniques [79–82]. Groundwater potential zones have been delineated for the research region by grouping the interpreted layers based on weighted multi-influencing criteria and then allocating different potential zones to each group of interpreted layers. Ultimately, the overall effect of the graded multi-influencing elements was quantified using an overlay analysis on a GIS environment, resulting in the mapping of subsurface water potential zones in the research region [83,84]. There are five separate groundwater potential zones within this study area: high–very high, moderate–high, low–moderate, very low–low, and nil–very low [Figure 14].

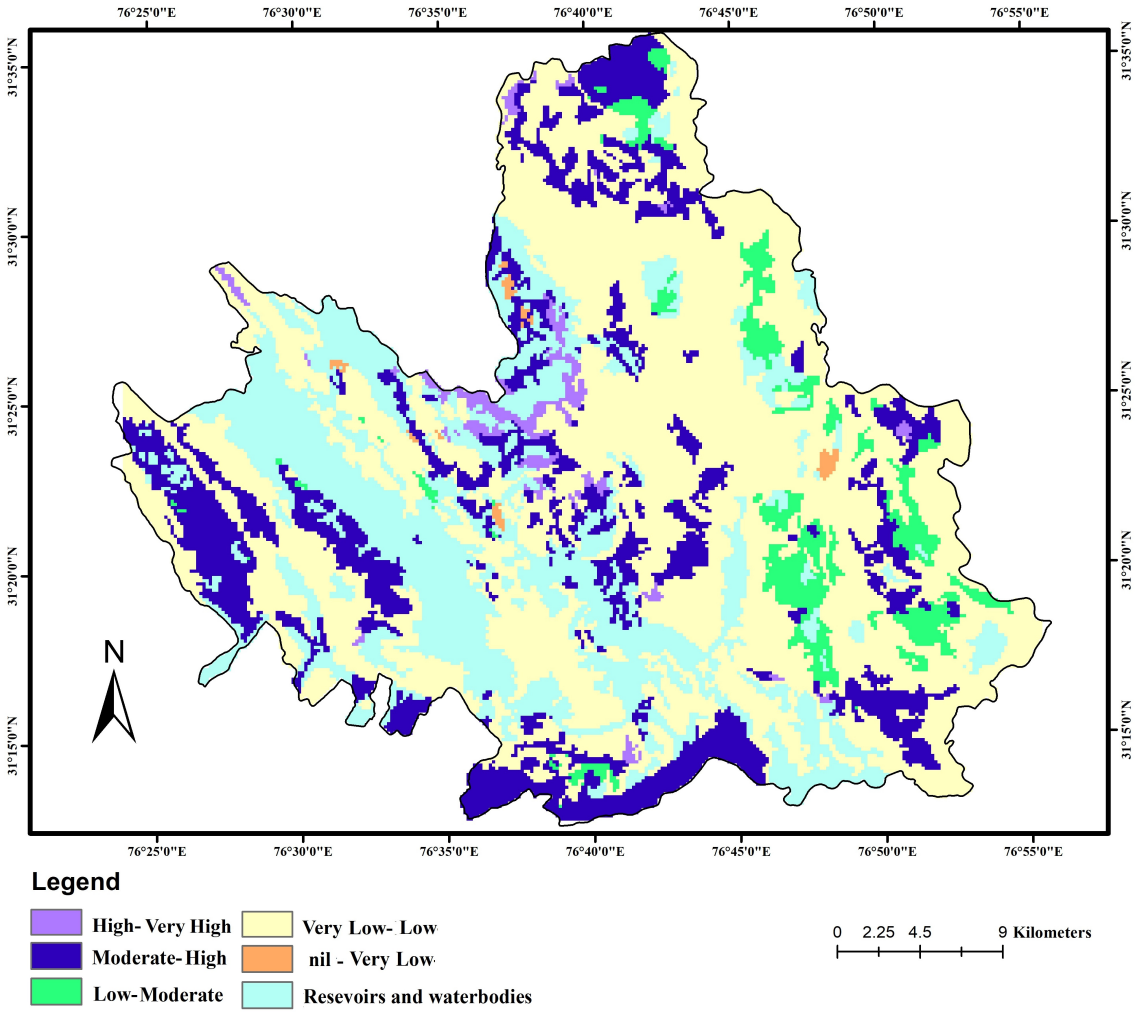

Figure 14. Groundwater potential zone map of study area, Bilaspur.

The maximum groundwater potential zone is located in the north-western sections of the research area where there is a large percentage of cropland with strong percolation capacity. This demonstrates that the texture of the soil and gradient have a substantial impact on groundwater enrichment. Furthermore, the concentration of drainage network, lithology and lineaments improves the groundwater system's capacity to fully infiltrate water. Of the overall study area, 0.33% is in the "nil–very low" zone, 51.64% is in the "very low–low" zone, 4.92% is in the "low–moderate" zone, 18.0% is in the "moderate–high" zone, and 25.0% is in the "high–very high" groundwater potential zone.

4.12. Validation

A model was used in the study to develop an output map that shows locations with a high potential for groundwater. By comparing it with information from field surveys and the CGWB report from 2020, the ground water potential map was verified (Figure 15).

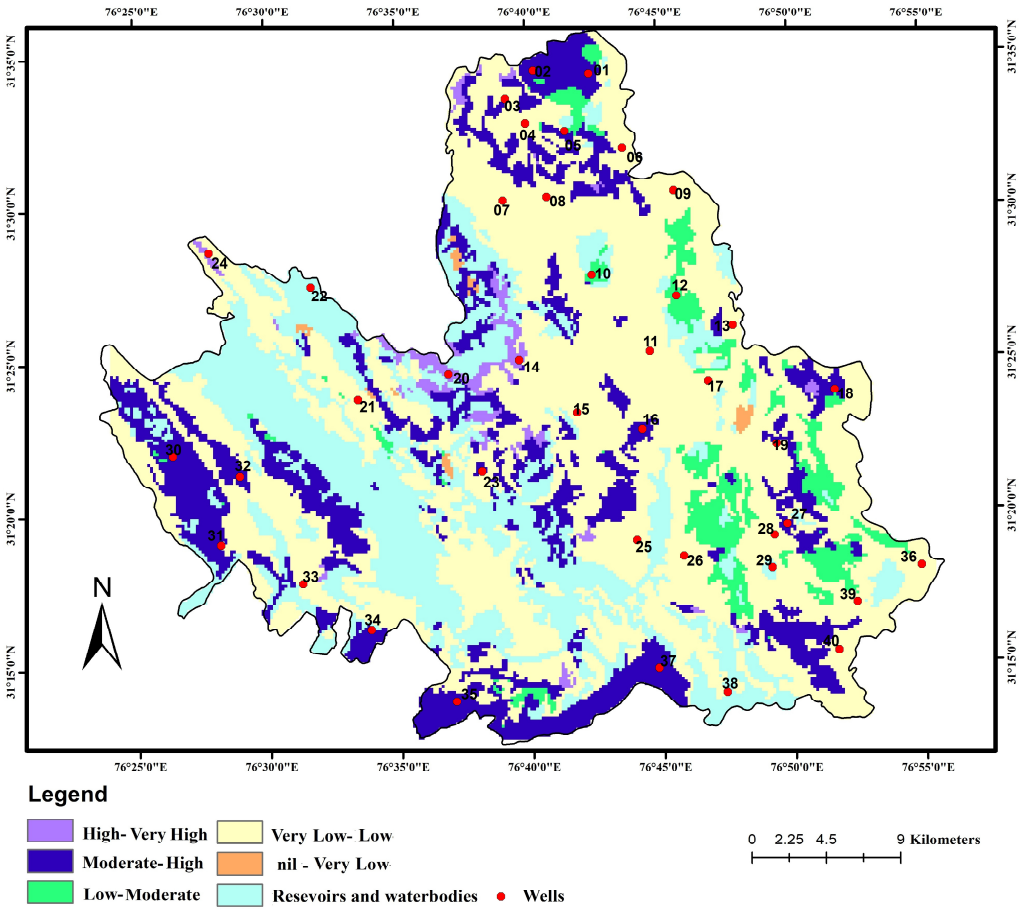

Figure 15. Groundwater potential zone map of study area, Bilaspur overlaid by the well location data.

The validation process employed in this study is a widely used technique for validating models that include success rates and predictions [85,86]. This method is useful for determining a model's statistical robustness and determining how well it predicts future events. To assess the model's capacity to predict outcomes based on the data it was trained on, we split the data in this study into two sets: one for modelling and the other for validation. To evaluate the model's predictive efficacy, 20% of the total data were randomly chosen from the validation set. The prospective index values were split into 100 classes, each with a cumulative interval of 1%, and plotted on a graph to create the success rate curve (SRC) and prediction rate curve (PRC) [87–90] (Figure 16). The PRC assesses the model's accuracy in making future predictions, whereas the SRC displays the percentage of prospective areas that were accurately identified by the model [90–93]. The SRCs and PRCs generated can be compared and evaluated using the AUC as a useful statistic [85]. The accuracy of the model's capacity to forecast the groundwater potential in the training dataset is shown by the AUC for the success rate curve, with a value of 1 denoting a perfect model and 0.5 denoting a model with no predictive power [88]. The success rate curve's AUC value in this study is 84.05 per cent, which shows that the model is highly accurate at predicting the groundwater potential in the training dataset. A higher AUC value indicates better predictive accuracy. The AUC for the prediction rate curve reflects the model's ability to forecast the groundwater potential in the test dataset [88]. The prediction rate curve's AUC value in this study is 79 per cent, which indicates that the model has respectable accuracy in forecasting the groundwater potential in the test dataset. It is crucial to remember that a variety of factors, including the calibre of the input data and the intricacy of the model, influence how accurate the forecasts are. Given that the study only employed data from readily accessible locations and time periods, the model's predicted accuracy may be constrained in this study by the quality of the input

data. The model's intricacy may also make it harder to generalise to areas with differing hydrogeological conditions. Future research should consider utilising more varied and substantial datasets and evaluating the model's correctness in various hydrogeological contexts [89–93]. Overall, even though the validation process utilised in this study offers a reliable way to assess how well the model predicts the future, care should be used when interpreting the AUC values and other metrics [94–97].

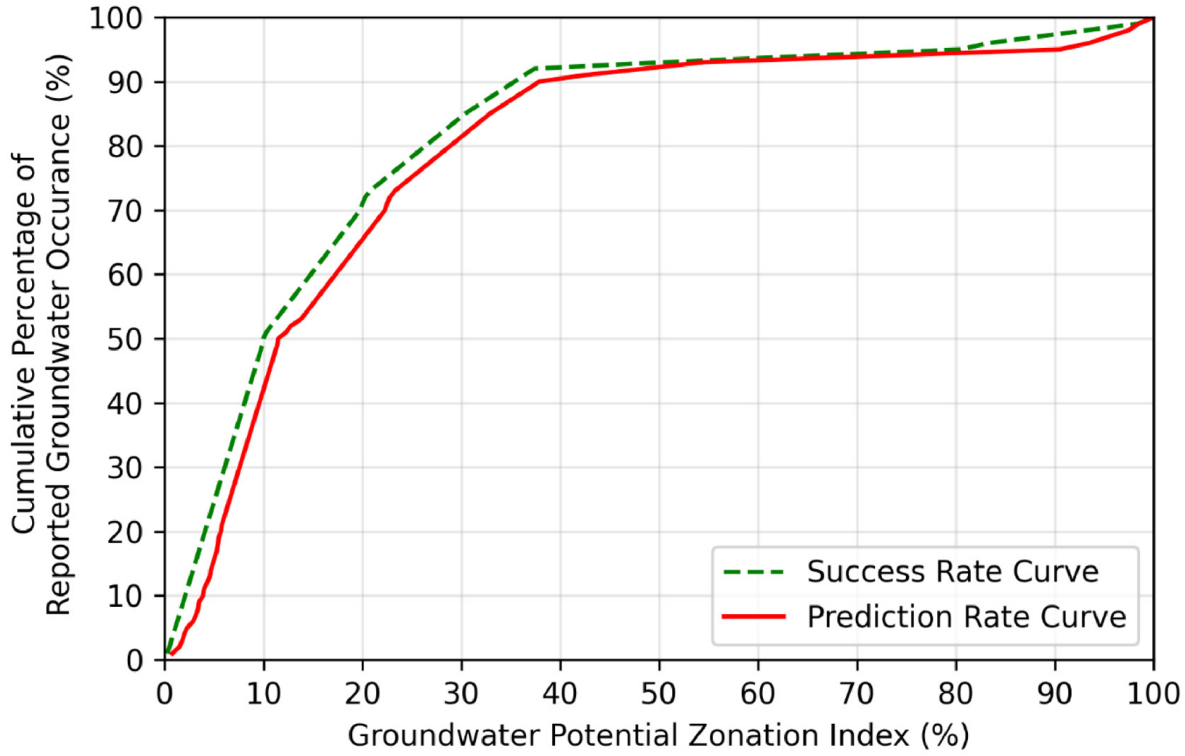

Figure 16. Groundwater potential zone map of study area, Bilaspur.

5. Conclusions

An effective tool for determining the availability of groundwater in the Himachal Pradesh region's Bilaspur region was the integration of GIS and remote sensing with the MIF approach. It is crucial to recognise the limits of this study, though. One drawback is the possibility of errors or flaws in the input data, which might affect how accurate the outcomes are. Another drawback is that the MIF technique only takes into account static parameters, neglecting dynamic elements such as groundwater recharge rates. It also depends on subjective judgments of the relative weights of different factors. Despite these drawbacks, the MIF strategy for determining groundwater availability proved to be more precise and effective than conventional expert-based strategies. Groundwater potential zones could be located utilising the thematic maps of the 10 influencing parameters made using satellite, meteorological, and auxiliary data. Additionally, the identification of suitable locations for subsurface water recharge structures was made possible by the classification of the groundwater potential zones into five categories based on the created output map. In order to validate the study, the accuracy of the model's predictions was tested using the success rate curve (SRC) and prediction rate curve (PRC) methodologies. The success rate curve's AUC value was discovered to be 84.05%, demonstrating a high degree of accuracy in forecasting groundwater potential in the training dataset. The prediction rate curve's AUC value was discovered to be 79 per cent, indicating a respectable level of accuracy in forecasting the groundwater potential in the test dataset. These findings offer additional proof of the validity and dependability of the suggested MIF approach for determining groundwater potential in the Himachal Pradesh region of Bilaspur. In light of this, it can be said that the integration of GIS and remote sensing with the MIF approach can be a useful

tool for finding and prioritising suitable places for groundwater recharge structures, which can aid in the long-term planning and management of water resources in the area. A quick and effective way to carry out MCDM in order to ascertain the availability of groundwater in a specific area is to use the MIF methodology in conjunction with GIS and remote sensing. Although this study has limitations, the approach offers promise for future studies and can contribute to the long-term planning and management of water resources.

Author Contributions: Conceptualisation, S.K.S., G.M. and S.K.; methodology, A.S., S.K.S., G.M., S., V.B. and P.K.; software, A.S., R.K., S.K.S., P.K. and G.M.; validation, A.S., R.K. and S.K.S.; formal analysis, A.S., R.K., S.K.S., S.K. and V.B.; investigation, A.S., R.K., S.K.S., P.K., S.K., A.R. and V.B.; resources, S.K.S. and S.K.; data curation, A.S., R.K., S.K.S. and G.M.; writing—original draft preparation A.S., R.K. and S.K.S.; writing—review and editing, A.S., R.K., S.K.S. and G.M.; visualisation, A.S., R.K., S.K.S., P.K., A.R. and G.M.; supervision, S.K.S. and S.K.; project administration, S.K.S. and S.K. All authors have read and agreed to the published version of the manuscript.

Funding: This research received no external funding.

Data Availability Statement: The data is available from corresponding authors upon reasonable request.

Acknowledgments: We would like to thank four anonymous reviewers whose constructive comments helped us to improve this manuscript manifold. We also acknowledge the help and support provided by the Central Ground Water Board, Himachal Pradesh for providing all the necessary information while collecting field samples. We are grateful to research scholar, Bhavneet Gulati for helping in collecting the field samples. The authors would like to thank Asif Marazi for helping in conducting the statistical validation part of this work using Python and R-statistical package.

Conflicts of Interest: The authors declare no conflict of interest.

References

1. Vereecken, H.; Amelung, W.; Bauke, S.L.; Bogena, H.; Brüggemann, N.; Montzka, C.; Vanderborght, J.; Bechtold, M.; Blöschl, G.; Carminati, A.; et al. Soil hydrology in the Earth system. *Nat. Rev. Earth Environ.* **2022**, *3*, 573–587. [CrossRef]
2. Zhang, K.; Li, H.; Han, J.; Jiang, B.; Gao, J. Understanding of mineral change mechanisms in coal mine groundwater reservoir and their influences on effluent water quality: A experimental study. *Int. J. Coal Sci. Technol.* **2021**, *8*, 154–167. [CrossRef]
3. Chilton, J. Groundwater Pollution—Developments in Water Science. In *Water Quality Assessments—A Guide to Use of Biota, Sediments and Water in Environmental Monitoring*, 2nd ed.; Chapman and Hall Ltd.: London, UK, 1996; Volume 5, p. 273.
4. Gibert, O.; Abenza, M.; Reig, M.; Vecino, X.; Sánchez, D.; Arnaldos, M.; Cortina, J.L. Removal of nitrate from groundwater by nano-scale zero-valent iron injection pulses in continuous-flow packed soil columns. *Sci. Total Environ.* **2022**, *810*, 152300. [CrossRef]
5. Harris, S.J.; Cendón, D.I.; Hankin, S.I.; Peterson, M.A.; Xiao, S.; Kelly, B.F. Isotopic evidence for nitrate sources and controls on denitrification in groundwater beneath an irrigated agricultural district. *Sci. Total Environ.* **2022**, *817*, 152606. [CrossRef]
6. Wang, X.; Xu, Y.J.; Zhang, L. Watershed scale spatiotemporal nitrogen transport and source tracing using dual isotopes among surface water, sediments and groundwater in the Yiluo River Watershed, Middle of China. *Sci. Total Environ.* **2022**, *833*, 155180. [CrossRef] [PubMed]
7. Singh, A.P.; Bhakar, P. Development of groundwater sustainability index: A case study of western arid region of Rajasthan, India. *Environ. Dev. Sustain.* **2021**, *23*, 1844–1868. [CrossRef]
8. Kumar, P.; Avtar, R.; Dasgupta, R.; Johnson, B.A.; Mukherjee, A.; Ahsan, M.N.; Nguyen, D.C.; Nguyen, H.Q.; Shaw, R.; Mishra, B.K. Socio-hydrology: A key approach for adaptation to water scarcity and achieving human well-being in large riverine islands. *Prog. Disaster Sci.* **2020**, *8*, 100134. [CrossRef]
9. Shyam, M.; Meraj, G.; Kanga, S.; Farooq, M.; Singh, S.K.; Sahu, N.; Kumar, P. Assessing the Groundwater Reserves of the Udaipur District, Aravalli Range, India, Using Geospatial Techniques. *Water* **2022**, *14*, 648. [CrossRef]
10. Meraj, G. Assessing the Impacts of Climate Change on Ecosystem Service Provisioning in Kashmir Valley India. Ph.D. Thesis, Suresh Gyan Vihar University, Jaipur, India, 2021.
11. Meraj, G.; Singh, S.K.; Kanga, S.; Islam, M.N. Modeling on comparison of ecosystem services concepts, tools, methods and their ecological-economic implications: A review. *Model. Earth Syst. Environ.* **2021**, *8*, 15–34. [CrossRef]
12. Upadhyay, M.K.; Majumdar, A.; Barla, A.; Bose, S.; Srivastava, S. An assessment of arsenic hazard in groundwater–soil–rice system in two villages of Nadia district, West Bengal, India. *Environ. Geochem. Health* **2019**, *41*, 2381–2395. [CrossRef]
13. Galkate, R.V.; Yadav, S.; Pandey, R.P.; Negm, A.M.; Yadava, R.N. An Overview: Water Resource Management Aspects in India. *Water Qual. Assess. Manag. India* **2022**, *16*, 29–55.
14. Prasad, R.K.; Mondal, N.C.; Banerjee, P.; Nandakumar, M.V.; Singh, V.S. Deciphering Potential Groundwater Zone in Hard Rock through the Application of GIS. *Environ. Geol.* **2008**, *55*, 467–475. [CrossRef]

15. Hamilton, P. Groundwater and Surface Water: A Single Resource. *Water Environ. Technol.* **2005**, *17*, 37–41.
16. Pradhan, B. Groundwater Potential Zonation for Basaltic Watersheds Using Satellite Remote Sensing Data and GIS Techniques. *Cent. Eur. J. Geosci.* **2009**, *1*, 120–129. [CrossRef]
17. Becker, M.W. Potential for Satellite Remote Sensing of Ground Water. *Groundwater* **2006**, *44*, 306–318. [CrossRef]
18. Rodell, M.; Famiglietti, J.S. The Potential for Satellite-Based Monitoring of Groundwater Storage Changes Using GRACE: The High Plains Aquifer, Central US. *J. Hydrol.* **2002**, *263*, 245–256. [CrossRef]
19. Li, W.; Fan, X.; Huang, F.; Chen, W.; Hong, H.; Huang, J.; Guo, Z. Uncertainties analysis of collapse susceptibility prediction based on remote sensing and GIS: Influences of different data-based models and connections between collapses and environmental factors. *Remote Sens.* **2020**, *12*, 4134. [CrossRef]
20. Rather, M.A.; Meraj, G.; Farooq, M.; Shiekh, B.A.; Kumar, P.; Kanga, S.; Singh, S.K.; Sahu, N.; Tiwari, S.P. Identifying the Potential Dam Sites to Avert the Risk of Catastrophic Floods in the Jhelum Basin, Kashmir, NW Himalaya, India. *Remote Sens.* **2022**, *14*, 1538. [CrossRef]
21. Abijith, D.; Saravanan, S.; Singh, L.; Jennifer, J.J.; Saranya, T.; Parthasarathy, K.S.S. GIS-Based Multi-Criteria Analysis for Identification of Potential Groundwater Recharge Zones—A Case Study from Ponnaniyaru Watershed, Tamil Nadu, India. *HydroResearch* **2020**, *3*, 1–14. [CrossRef]
22. Raju, R.S.; Raju, G.S.; Rajasekhar, M. Identification of Groundwater Potential Zones in Mandavi River Basin, Andhra Pradesh, India Using Remote Sensing, GIS and MIF Techniques. *HydroResearch* **2019**, *2*, 1–11. [CrossRef]
23. Ahmed, A.; Ranasinghe-Arachchilage, C.; Alrajhi, A.; Hewa, G. Comparison of Multicriteria Decision-Making Tech-niques for Groundwater Recharge Potential Zonation: Case Study of the Willochra Basin, South Australia. *Water* **2021**, *13*, 525. [CrossRef]
24. Anbarasu, S.; Brindha, K.; Elango, L. Multi-influencing factor method for delineation of groundwater potential zones using remote sensing and GIS techniques in the western part of Perambalur district, southern India. *Earth Sci. Inform.* **2020**, *13*, 317–332. [CrossRef]
25. Roy, S.; Hazra, S.; Chanda, A.; Das, S. Assessment of Groundwater Potential Zones Using Multi-Criteria Deci-sion-Making Technique: A Micro-Level Case Study from Red and Lateritic Zone (RLZ) of West Bengal, India. *Sustain. Water Resour. Manag.* **2020**, *6*, 4. [CrossRef]
26. Pourghasemi, H.R.; Beheshtirad, M. Assessment of a Data-Driven Evidential Belief Function Model and GIS for Groundwater Potential Mapping in the Koohrang Watershed, Iran. *Geocarto Int.* **2015**, *30*, 662–685. [CrossRef]
27. Sander, P. Lineaments in Groundwater Exploration: A Review of Applications and Limitations. *Hydrogeol. J.* **2007**, *15*, 71–74. [CrossRef]
28. Nag, S.K.; Ray, S. Deciphering Groundwater Potential Zones Using Geospatial Technology: A Study in Bankura Block I and Block II, Bankura District, West Bengal. *Arab. J. Sci. Eng.* **2015**, *40*, 205–214. [CrossRef]
29. Singh, D.K.; Singh, A.K. Groundwater Situation in India: Problems and Perspective. *Int. J. Water Resour. Dev.* **2002**, *18*, 563–580. [CrossRef]
30. Singh, L.K.; Jha, M.K.; Chowdary, V.M. Assessing the Accuracy of GIS-Based Multi-Criteria Decision Analysis Ap-proaches for Mapping Groundwater Potential. *Ecol. Indic.* **2018**, *91*, 24–37. [CrossRef]
31. Thapa, R.; Gupta, S.; Guin, S.; Kaur, H. Assessment of Groundwater Potential Zones Using Multi-Influencing Factor (MIF) and GIS: A Case Study from Birbhum District, West Bengal. *Appl. Water Sci.* **2017**, *7*, 4117–4131. [CrossRef]
32. Fagbohun, B.J. Integrating GIS and Multi-Influencing Factor Technique for Delineation of Potential Groundwater Recharge Zones in Parts of Ilesha Schist Belt, Southwestern Nigeria. *Environ. Earth Sci.* **2018**, *77*, 69. [CrossRef]
33. Oikonomidis, D.; Dimogianni, S.; Kazakis, N.; Voudouris, K. A GIS/Remote Sensing-Based Methodology for Groundwater Potentiality Assessment in Tirnavos Area, Greece. *J. Hydrol.* **2015**, *525*, 197–208. [CrossRef]
34. Owolabi, S.T.; Madi, K.; Kalumba, A.M.; Orimoloye, I.R. A Groundwater Potential Zone Mapping Approach for Semi-Arid Environments Using Remote Sensing (RS), Geographic Information System (GIS), and Analytical Hierarchical Process (AHP) Techniques: A Case Study of Buffalo Catchment, Eastern Cape, South Africa. Arab. *J. Geosci.* **2020**, *13*, 1184. [CrossRef]
35. Tolche, A.D. Groundwater Potential Mapping Using Geospatial Techniques: A Case Study of Dhungeta-Ramis Sub-Basin, Ethiopia. *Geol. Ecol. Landsc.* **2021**, *5*, 65–80. [CrossRef]
36. Yeh, H.F.; Cheng, Y.S.; Lin, H.I.; Lee, C.H. Mapping Groundwater Recharge Potential Zone Using a GIS Approach in Hualian River, Taiwan. *Sustain. Environ. Res.* **2016**, *26*, 33–43. [CrossRef]
37. Zghibi, A.; Mirchi, A.; Msaddek, M.H.; Merzougui, A.; Zouhri, L.; Taupin, J.D.; Chekirbane, A.; Chenini, I.; Tarhouni, J. Using Analytical Hierarchy Process and Multi-Influencing Factors to Map Groundwater Recharge Zones in a Semi-Arid Mediterranean. *Water* **2020**, *12*, 2525. [CrossRef]
38. Pradhan, A.M.; Kim, Y.T.; Shrestha, S.; Huynh, T.C.; Nguyen, B.P. Application of deep neural network to capture groundwater potential zone in mountainous terrain, Nepal Himalaya. *Environ. Sci. Pollut. Res.* **2021**, *28*, 18501–18517. [CrossRef] [PubMed]
39. Nasir, M.J.; Khan, S.; Ayaz, T.; Khan, A.Z.; Ahmad, W.; Lei, M. An Integrated Geospatial Multi-Influencing Factor Approach to Delineate and Identify Groundwater Potential Zones in Kabul Province, Afghanistan. *Environ. Earth Sci.* **2021**, *80*, 453. [CrossRef]
40. Jhariya, D.C.; Kumar, T.; Gobinath, M.; Diwan, P.; Kishore, N. Assessment of Groundwater Potential Zone Using Remote Sensing, GIS and Multi Criteria Decision Analysis Techniques. *J. Geol. Soc. India* **2016**, *88*, 481–492. [CrossRef]
41. Magesh, N.S.; Chandrasekar, N.; Soundranayagam, J.P. Delineation of Groundwater Potential Zones in Theni District, Tamil Nadu, Using Remote Sensing, GIS and MIF Techniques. *Geosci. Front.* **2012**, *3*, 189–196. [CrossRef]

42. Arkoprovo, B.; Adarsa, J.; Animesh, M. Application of Remote Sensing, GIS and MIF Technique for Elucidation of Groundwater Potential Zones from a Part of Orissa Coastal Tract, Eastern India. *Res. J. Recent Sci.* **2013**, *2*, 42–49.
43. Bhattacharya, S.; Das, S.; Das, S.; Kalashetty, M.; Warghat, S.R. An Integrated Approach for Mapping Groundwater Potential Applying Geospatial and MIF Techniques in the Semiarid Region. *Environ. Dev. Sustain.* **2021**, *23*, 495–510. [CrossRef]
44. Das, S.; Gupta, A.; Ghosh, S. Exploring Groundwater Potential Zones Using MIF Technique in Semi-Arid Region: A Case Study of Hingoli District, Maharashtra. *Spat. Inf. Res.* **2017**, *25*, 749–756. [CrossRef]
45. Bhuvaneswaran, C.; Ganesh, A.; Nevedita, S. Spatial Analysis of Groundwater Potential Zones Using Remote Sensing, GIS and MIF Techniques in Uppar Odai Sub-Watershed, Nandiyar, Cauvery Basin, Tamilnadu. *Int. J. Curr. Res.* **2015**, *7*, 20765–20774.
46. Singha, S.; Pasupuleti, S.; Durbha, K.S.; Singha, S.S.; Singh, R.; Venkatesh, A.S. An analytical hierarchy process-based geospatial modeling for delineation of potential anthropogenic contamination zones of groundwater from Arang block of Raipur district, Chhattisgarh, Central India. *Environ. Earth Sci.* **2019**, *78*, 1–9. [CrossRef]
47. Dwivedi, C.S.; Raza, R.; Mitra, D.; Pandey, A.C.; Jhariya, D.C. Groundwater potential zone delineation in hard rock terrain for sustainable groundwater development and management in South Madhya Pradesh, India. *Geogr. Environ. Sustain.* **2021**, *14*, 106–121. [CrossRef]
48. Sud, A. Delineation of Groundwater Potential Zone Using the Integration of Geospatial Model and Multi Influencing Factor (MIF) Decision Making Technique: A Review. *SGVU J. Clim. Chang. Water* **2021**, *8*, 1–13.
49. Kumar, S.; Shruti, S.; Shailja, K.; Mishra, K. Delineation of Groundwater Potential Zone Using Geospatial Techniques for Shimla City, Himachal Pradesh (India). *Int. J. Sci. Res. Dev.* **2017**, *5*, 225–234.
50. Chauhan, N.S. *Medicinal and Aromatic Plants of Himachal Pradesh*; Indus Publishing: New Delhi, India, 1999.
51. Upgupta, S.; Sharma, J.; Jayaraman, M.; Kumar, V.; Ravindranath, N.H. Climate change impact and vulnerability assessment of forests in the Indian Western Himalayan region: A case study of Himachal Pradesh, India. *Clim. Risk Manag.* **2015**, *10*, 63–67. [CrossRef]
52. Prasher, R.S.; Devi, N. Agricultural diversification in Himachal Pradesh: An economic analysis. *Indian J. Econ. Dev.* **2018**, *6*, 1–6.
53. Dev, R.; Bali, M. Evaluation of groundwater quality and its suitability for drinking and agricultural use in district Kangra of Himachal Pradesh, India. *J. Saudi Soc. Agric. Sci.* **2019**, *18*, 462–468. [CrossRef]
54. Parihar, S. Salvaging, Transplantation and Reconstruction of Heritage Sites, Techniques and Problems: A Study of the Submerged Temple of Bilaspur District in Himachal Pradesh. *Indian Hist. Rev.* **2019**, *46*, 167–183. [CrossRef]
55. Singh, S.; Dhasmana, M.K.; Shrivastava, V.; Sharma, V.; Pokhriyal, N.; Thakur, P.K.; Aggarwal, S.P.; Nikam, B.R.; Garg, V.; Chouksey, A.; et al. Estimation of revised capacity in Gobind Sagar reservoir using Google earth engine and GIS. *Int. Arch. Photogramm. Remote Sens. Spat. Inf. Sci.* **2018**, *42*. [CrossRef]
56. Kanga, S.; Singh, S.K.; Meraj, G.; Kumar, A.; Parveen, R.; Kranjčić, N.; Đurin, B. Assessment of the impact of urbanization on geoenvironmental settings using geospatial techniques: A study of Panchkula District, Haryana. *Geographies* **2022**, *2*, 1–10. [CrossRef]
57. Hudson, P.F.; Colditz, R.R.; Aguilar-Robledo, M. Spatial relations between floodplain environments and land use–land cover of a large lowland tropical river valley: Panuco basin, Mexico. *Environ. Manag.* **2006**, *38*, 487–503. [CrossRef] [PubMed]
58. Meraj, G.; Farooq, M.; Singh, S.K.; Islam, M.N.; Kanga, S. Modeling the sediment retention and ecosystem provisioning services in the Kashmir valley, India, Western Himalayas. *Model. Earth Syst. Environ.* **2022**, *8*, 3859–3884. [CrossRef]
59. Lahon, D.; Sahariah, D.; Debnath, J.; Nath, N.; Meraj, G.; Farooq, M.; Kanga, S.; Singh, S.; Chand, K. Growth of water hyacinth biomass and its impact on the floristic composition of aquatic plants in a wetland ecosystem of the Brahmaputra floodplain of Assam, India. *PeerJ* **2023**, *11*, e14811. [CrossRef]
60. Nath, N.; Sahariah, D.; Meraj, G.; Debnath, J.; Kumar, P.; Lahon, D.; Chand, K.; Farooq, M.; Chandan, P.; Singh, S.K.; et al. Land Use and Land Cover Change Monitoring and Prediction of a UNESCO World Heritage Site: Kaziranga Eco-Sensitive Zone Using Cellular Automata-Markov Model. *Land* **2023**, *12*, 151. [CrossRef]
61. Kanga, S.; Meraj, G.; Johnson, B.A.; Singh, S.K.; PV, M.N.; Farooq, M.; Kumar, P.; Marazi, A.; Sahu, N. Understanding the Linkage between Urban Growth and Land Surface Temperature—A Case Study of Bangalore City, India. *Remote Sens.* **2022**, *14*, 4241. [CrossRef]
62. Meraj, G.; Romshoo, S.A.; Yousuf, A.R.; Altaf, S.; Altaf, F. Assessing the influence of watershed characteristics on the flood vulnerability of Jhelum basin in Kashmir Himalaya. *Nat. Hazards* **2015**, *77*, 153–175. [CrossRef]
63. Masoud, A.; Koike, K. Applicability of computer-aided comprehensive tool (LINDA: Lineament Detection and Analysis) and shaded digital elevation model for characterizing and interpreting morphotectonic features from lineaments. *Comput. Geosci.* **2017**, *106*, 89–100. [CrossRef]
64. Soliman, A.; Han, L. Effects of vertical accuracy of digital elevation model (DEM) data on automatic lineaments extraction from shaded DEM. *Adv. Space Res.* **2019**, *64*, 603–622. [CrossRef]
65. Altaf, F.; Meraj, G.; Romshoo, S.A. Morphometric analysis to infer hydrological behaviour of Lidder watershed, Western Himalaya, India. *Geogr. J.* **2013**, *2013*, 178021. [CrossRef]
66. Meraj, G.; Yousuf, A.R.; Romshoo, S.A. Impacts of the Geo-Environmental Setting on the Flood Vulnerability at Watershed Scale in the Jhelum Basin. Master's Thesis, University of Kashmir, Srinagar, India, 2013.
67. Altaf, S.; Meraj, G.; Romshoo, S.A. Morphometry and land cover based multi-criteria analysis for assessing the soil erosion susceptibility of the western Himalayan watershed. *Environ. Monit. Assess.* **2014**, *186*, 8391–8412. [CrossRef] [PubMed]

68. Ollier, C.D.; Thomasson, A.J. Asymmetrical valleys of the Chiltern Hills. *Geogr. J.* **1957**, *123*, 71–80. [CrossRef]
69. Jackson, M.; Roering, J.J. Post-fire geomorphic response in steep, forested landscapes: Oregon Coast Range, USA. *Quat. Sci. Rev.* **2009**, *28*, 1131–1146. [CrossRef]
70. Debnath, J.; Meraj, G.; Das Pan, N.; Chand, K.; Debbarma, S.; Sahariah, D.; Gualtieri, C.; Kanga, S.; Singh, S.K.; Farooq, M.; et al. Integrated remote sensing and field-based approach to assess the temporal evolution and future projection of meanders: A case study on River Manu in North-Eastern India. *PLoS ONE* **2022**, *17*, e0271190. [CrossRef]
71. Roy, P.K.; Basak, S.K.; Mohinuddin, S.; Roy, M.B.; Halder, S.; Ghosh, T. Modelling groundwater potential zone using fuzzy logic and geospatial technology of an deltaic island. *Model. Earth Syst. Environ.* **2022**, *8*, 5565–5584. [CrossRef]
72. Navale, V.; Mhaske, S. Artificial Neural Network (ANN) and Adaptive Neuro-Fuzzy Inference System (ANFIS) model for Forecasting Groundwater Level in the Pravara River Basin, India. *Model. Earth Syst. Environ.* **2022**, *27*, 1–4. [CrossRef]
73. Wirth, S.B.; Carlier, C.; Cochand, F.; Hunkeler, D.; Brunner, P. Lithological and tectonic control on groundwater contribution to stream discharge during low-flow conditions. *Water* **2020**, *12*, 821. [CrossRef]
74. Singh, M.; Hartsch, K. Basics of soil erosion. In *Watershed Hydrology, Management and Modeling*; CRC Press: Boca Raton, FL, USA, 2019; Volume 31, pp. 1–61.
75. Misra, D.K.; Tewari, V.C. Tectonics and sedimentation of the rocks between Mandi and Rohtang, Beas valley, Himachal Pradesh, India. *Geosci. J.* **1988**, *9*, 153–172.
76. Srivastava, P.; Patel, S.; Singh, N.; Jamir, T.; Kumar, N.; Aruche, M.; Patel, R.C. Early Oligocene paleosols of the Dagshai Formation, India: A record of the oldest tropical weathering in the Himalayan foreland. *Sediment. Geol.* **2013**, *294*, 142–156. [CrossRef]
77. Rahimi-Aghdam, S.; Chau, V.T.; Lee, H.; Nguyen, H.; Li, W.; Karra, S.; Rougier, E.; Viswanathan, H.; Srinivasan, G.; Bažant, Z.P. Branching of hydraulic cracks enabling permeability of gas or oil shale with closed natural fractures. *Proc. Natl. Acad. Sci. USA* **2019**, *116*, 1532–1537. [CrossRef] [PubMed]
78. Grenfell, S.; Grenfell, M.; Ellery, W.; Job, N.; Walters, D. A genetic geomorphic classification system for southern African palustrine wetlands: Global implications for the management of wetlands in drylands. *Front. Environ. Sci.* **2019**, *7*, 174. [CrossRef]
79. Roy, S.; Bose, A.; Mandal, G. Modeling and mapping geospatial distribution of groundwater potential zones in Darjeeling Himalayan region of India using analytical hierarchy process and GIS technique. *Model. Earth Syst. Environ.* **2022**, *8*, 1563–1584. [CrossRef]
80. Meraj, G.; Romshoo, S.A.; Ayoub, S.; Altaf, S. Geoinformatics based approach for estimating the sediment yield of the mountainous watersheds in Kashmir Himalaya, India. *Geocarto Int.* **2018**, *33*, 1114–1138. [CrossRef]
81. Fayaz, M.; Meraj, G.; Khader, S.A.; Farooq, M. ARIMA and SPSS statistics based assessment of landslide occurrence in western Himalayas. *Environ. Chall.* **2022**, *9*, 100624. [CrossRef]
82. Fayaz, M.; Meraj, G.; Khader, S.A.; Farooq, M.; Kanga, S.; Singh, S.K.; Kumar, P.; Sahu, N. Management of landslides in a rural–urban transition zone using machine learning algorithms—A case study of a National Highway (NH-44), India, in the Rugged Himalayan Terrains. *Land* **2022**, *11*, 884. [CrossRef]
83. Rehman, A.; Song, J.; Haq, F.; Mahmood, S.; Ahamad, M.I.; Basharat, M.; Sajid, M.; Mehmood, M.S. Multi-hazard susceptibility assessment using the analytical hierarchy process and frequency ratio techniques in the Northwest Himalayas, Pakistan. *Remote Sens.* **2022**, *14*, 554. [CrossRef]
84. Islam, F.; Ahmad, M.N.; Janjuhah, H.T.; Ullah, M.; Islam, I.U.; Kontakiotis, G.; Skilodimou, H.D.; Bathrellos, G.D. Modelling and Mapping of Soil Erosion Susceptibility of Murree, Sub-Himalayas Using GIS and RS-Based Models. *Appl. Sci.* **2022**, *12*, 12211. [CrossRef]
85. Post, D.E.; Votta, L.G. Computational science demands a new paradigm. *Phys. Today* **2005**, *58*, 35–41. [CrossRef]
86. Rasha, K.M. Salinity Prediction at the Bhairab River in the South-Western Part of Bangladesh Using Artificial Neural Network. *Nat. Environ. Pollut. Technol.* **2022**, *21*, 1431–1438. [CrossRef]
87. Wang, G.; Chen, X.; Chen, W. Spatial prediction of landslide susceptibility based on GIS and discriminant functions. *ISPRS Int. J. Geo Inf.* **2020**, *9*, 144. [CrossRef]
88. Yi, Y.; Zhang, Z.; Zhang, W.; Jia, H.; Zhang, J. Landslide susceptibility mapping using multiscale sampling strategy and convolutional neural network: A case study in Jiuzhaigou region. *Catena* **2020**, *195*, 104851. [CrossRef]
89. Arabameri, A.; Saha, S.; Chen, W.; Roy, J.; Pradhan, B.; Bui, D.T. Flash flood susceptibility modelling using functional tree and hybrid ensemble techniques. *J. Hydrol.* **2020**, *587*, 125007. [CrossRef]
90. Chen, Z.; Song, D.; Juliev, M.; Pourghasemi, H.R. Landslide susceptibility mapping using statistical bivariate models and their hybrid with normalized spatial-correlated scale index and weighted calibrated landslide potential model. *Environ. Earth Sci.* **2021**, *80*, 1–9. [CrossRef]
91. Lee, S.; Hong, S.M.; Jung, H.S. GIS-Based Groundwater Potential Mapping Using Artificial Neural Network and Support Vector Machine Models: The Case of Boryeong City in Korea. *Geocarto Int.* **2018**, *33*, 847–861. [CrossRef]
92. Sener, E.; Davraz, A.; Ozcelik, M. An Integration of GIS and Remote Sensing in Groundwater Investigations: A Case Study in Burdur, Turkey. *Hydrogeol. J.* **2005**, *13*, 826–834. [CrossRef]
93. Arulbalaji, P.; Padmalal, D.; Sreelash, K. GIS and AHP Techniques Based Delineation of Groundwater Potential Zones: A Case Study from Southern Western Ghats, India. *Sci. Rep.* **2019**, *9*, 2082. [CrossRef]

94. Sashikkumar, M.C.; Selvam, S.; Kalyanasundaram, V.L.; Johnny, J.C. GIS Based Groundwater Modeling Study to Assess the Effect of Artificial Recharge: A Case Study from Kodaganar River Basin, Dindigul District, Tamil Nadu. *J. Geol. Soc. India* **2017**, *89*, 57–64. [CrossRef]
95. Lee, S.; Hyun, Y.; Lee, S.; Lee, M.J. Groundwater potential mapping using remote sensing and GIS-based machine learning techniques. *Remote Sens.* **2020**, *12*, 1200. [CrossRef]
96. Mandal, U.; Sahoo, S.; Munusamy, S.B.; Dhar, A.; Panda, S.N.; Kar, A.; Mishra, P.K. Delineation of Groundwater Potential Zones of Coastal Groundwater Basin Using Multi-Criteria Decision Making Technique. *Water Resour. Manag.* **2016**, *30*, 4293–4310. [CrossRef]
97. Selvarani, A.G.; Elangovan, K.; Kumar, C.S. Evaluation of Groundwater Potential Zones Using Electrical Resistivity and GIS in Noyyal River Basin, Tamil Nadu. *J. Geol. Soc. India* **2016**, *87*, 573–582. [CrossRef]